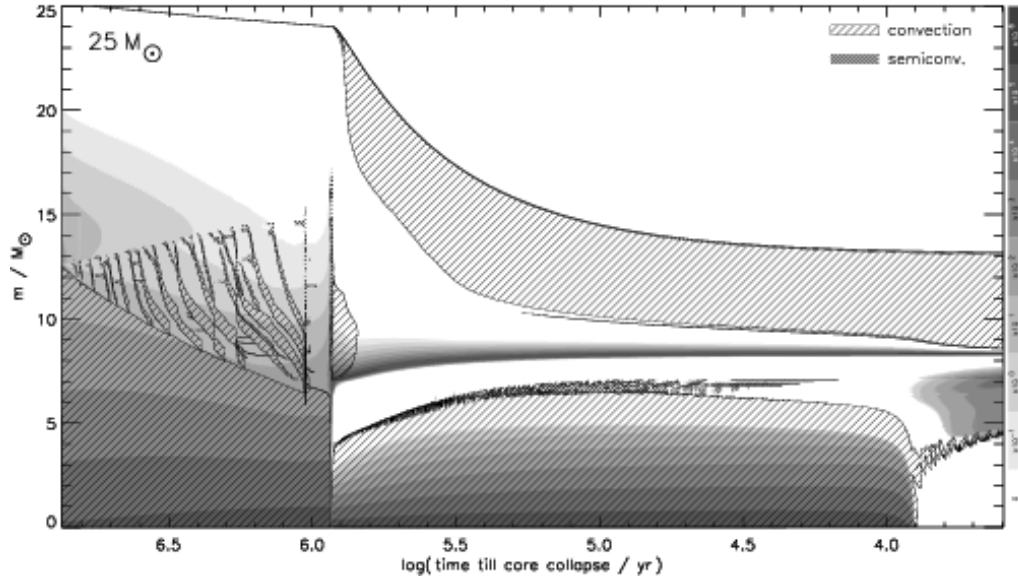
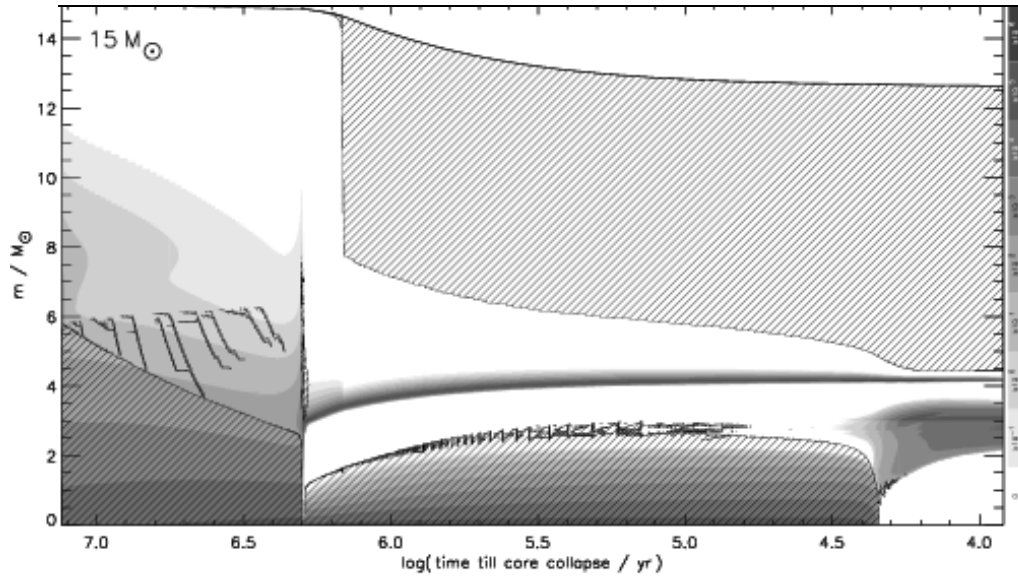


Lecture 8

*Overshoot Mixing,
Semiconvection, Mass Loss,
and Rotation*



The three greatest uncertainties in modeling stars, especially the presupernova evolution of single massive stars are:

- Convection and convective boundaries (undershoot, overshoot, semiconvection, late stages)
- The effects of rotation
- Mass loss (and its dependence on metallicity)

Convective Overshoot (and Undershoot) Mixing

Initially the entropy is nearly flat in a zero age main sequence star so just where convection stops is a bit ambiguous. As burning proceeds and the entropy decreases in the center, the convective extent becomes more precisely defined. Still one expects some “fuzziness” in the boundary. Convective plumes should not stop at a precisely determined point and entropy as a function of radius may vary with angle. Multi-D calculations of entire burning stages are not feasible.

A widely adopted prescription is to continue arbitrarily the convective mixing beyond its mathematical boundary by some fraction, a , of the pressure scale height. Maeder uses 20%. Stothers and Chin (ApJ, 381, L67), based on the width of the main sequence, argue that a is less than about 20%. Doom, Chiosi, and many European groups once used larger values. Woosley and Heger use much less. Nomoto et al use none.

This is an area where multi-dimensional simulation may make progress in the next decade.

Some references:

DeMarque et al, *ApJ*, **426**, 165, (1994) – modeling main sequence widths in clusters suggests $\alpha = 0.23$

Woo and Demarque, *AJ*, **122**, 1602 (2001) – empirically for low mass stars, overshoot is $< 15\%$ of the core radius. Core radius a better discriminant than pressure scale height.

Brumme, Clune, and Toomre, *ApJ*, **570**, 825, (2002) – numerical 3D simulations. Overshoot may go a significant fraction of a pressure scale height, but does not quickly establish an adiabatic gradient in the region.

Meakin and Arnett, *ApJ*,. **667**, 448 (2007) – treats overshoot mixing as an entrainment process sensitive to the Richardson number

Differential rotation complicates things and may have some of the same effects as overshoot.

Convective Overshoot

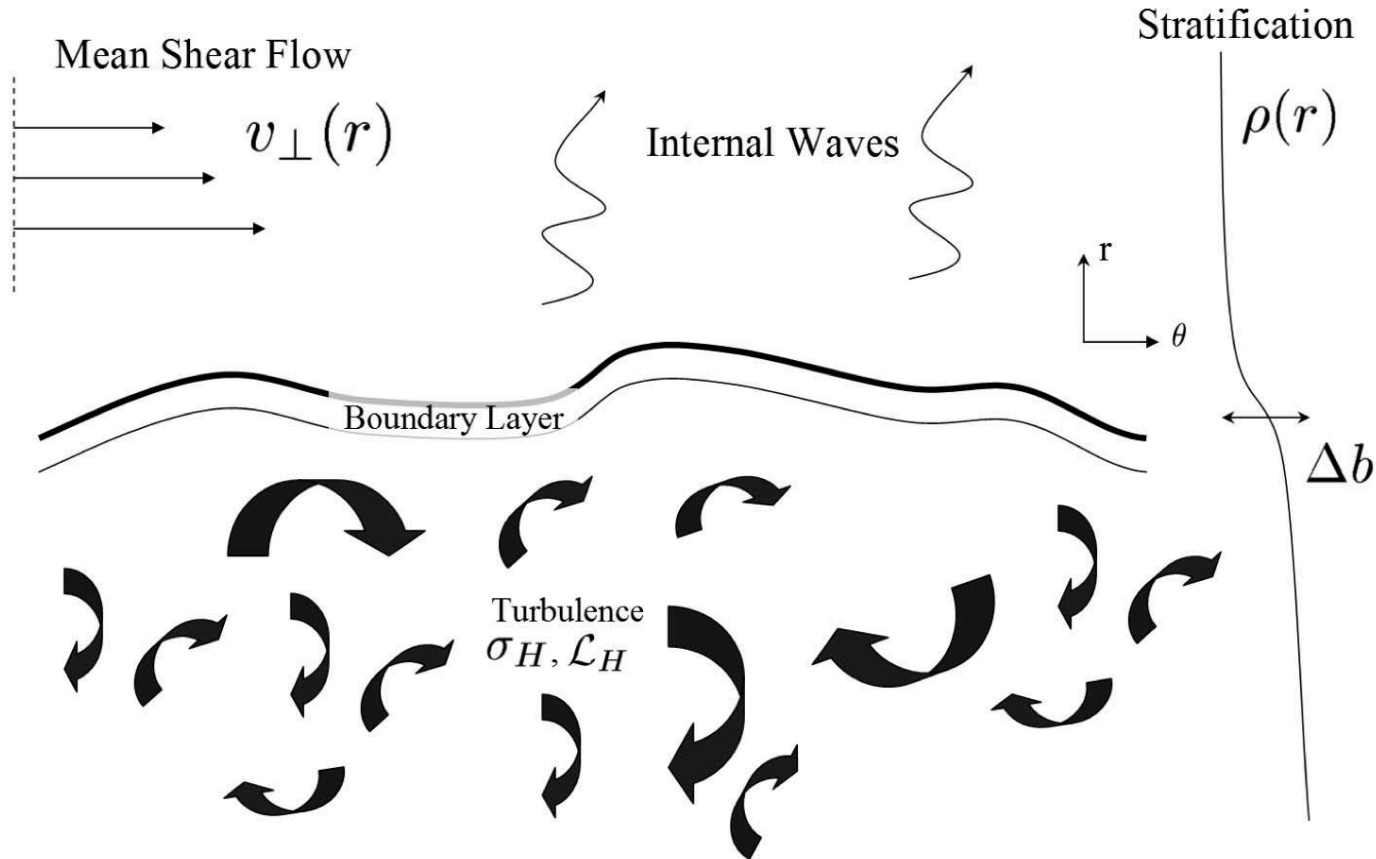
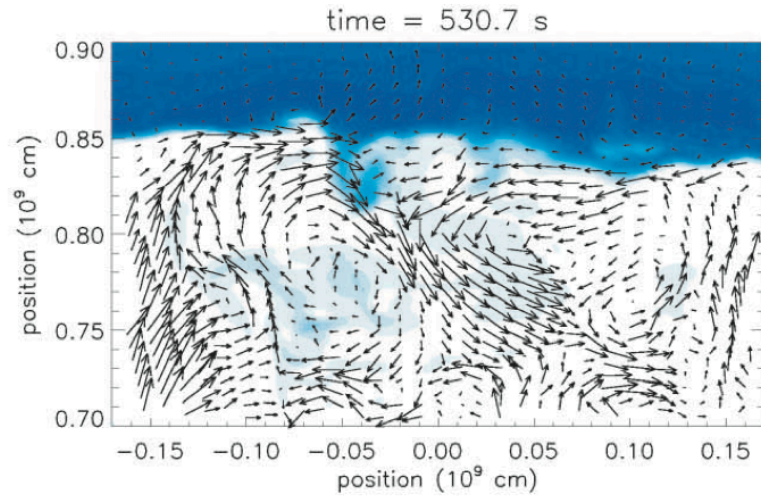
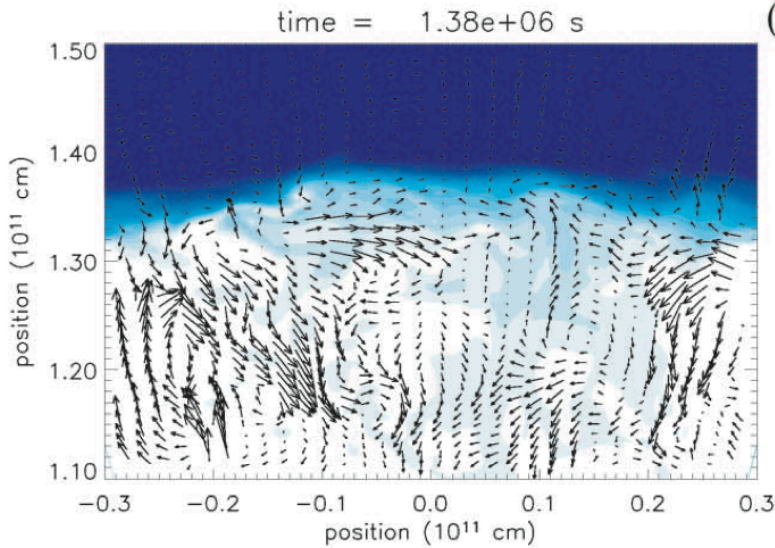
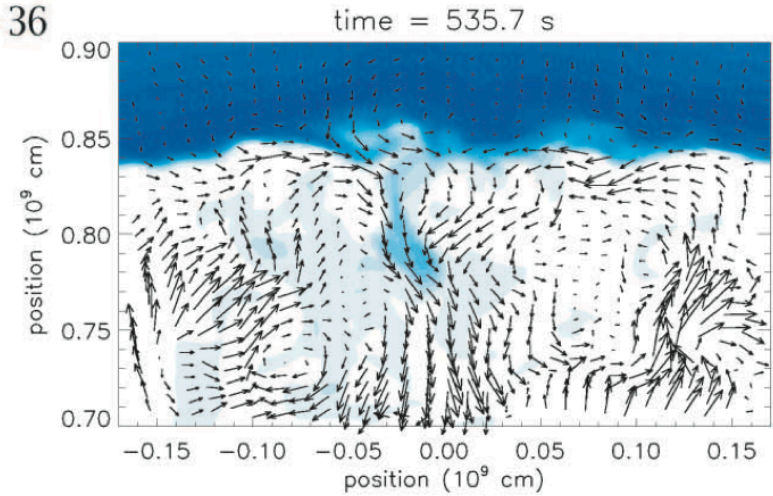
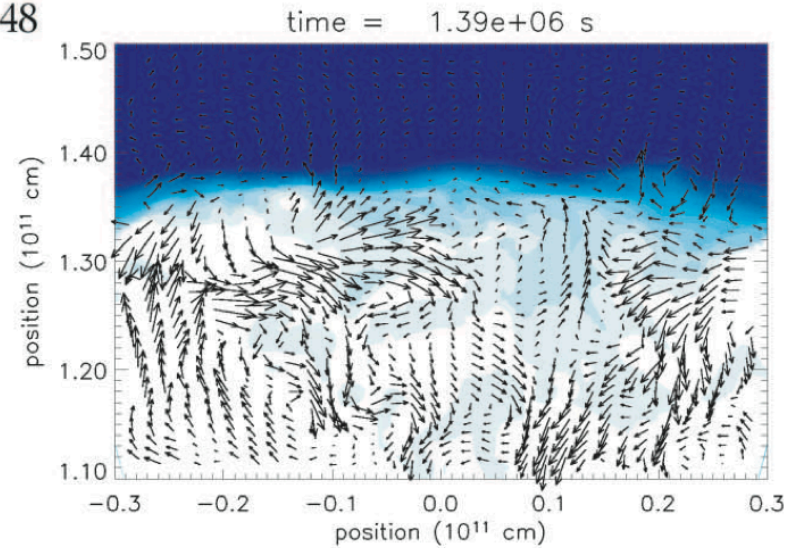


FIG. 1.—Diagram illustrating the salient features of the density and velocity field for the turbulent entrainment problem. Three layers are present: a turbulent convection zone is separated from an overlying stably stratified region by a boundary layer of thickness h and buoyancy jump $\Delta b \sim N^2 h$. The turbulence near the interface is characterized by integral scale and rms velocity \mathcal{L}_H and σ_H , respectively. The stably stratified layer with buoyancy frequency $N(r)$ propagates internal waves that are excited by the adjacent turbulence. A shear velocity field $v_{\perp}(r)$, associated with differential rotation, may also be present. After Strang & Fernando (2001).

(a) $Ri = 36$ (b) $Ri = 48$ 

Entrainment given by the Richardson number
See paper for functional dependence.

$Ri = \frac{\Delta b L}{\sigma^2}$ where Δb is the change in buoyancy, L , the length scale and σ^2 the turbulent velocity dispersion adjacent to the interface.

Overshoot mixing is important for

- Setting the size of the cores, especially CO cores, in the advanced evolution of massive stars
- Altering the luminosity and lifetime on the main sequence
- Allowing interpenetration of hydrogen and helium in the thin helium shell flashes in AGB stars
- Mixing in the sun at the tachyocline
- Dredge up of H in classical nova outbursts
- Decrease in critical mass for C ignition
- and more ...

Current work is in progress at UCSC.

Semiconvection

A historical split in the way convection is treated in a stellar evolution code comes about because the adiabatic condition can be written two ways – one based on the temperature gradient, the other on the density gradient.

From the first law of thermodynamics - Non-degenerate gas (Clayton 118ff):

$$0 = dQ = TdS = \left(\frac{\partial U}{\partial T} \right)_V dT + \left(\frac{\partial U}{\partial V} \right)_T dV + PdV \quad V \equiv \frac{1}{\rho}$$

$$U = aT^4V + \frac{3}{2} \frac{N_A}{\mu} kT \quad P = \frac{1}{3} aT^4 + \frac{N_A}{\mu V} kT$$

Ignoring μ -dependence:

$$\Gamma_1 = \frac{32 - 24\beta - 3\beta^2}{24 - 21\beta}$$

$$\Gamma_2 = \frac{32 - 24\beta - 3\beta^2}{24 - 18\beta - 3\beta^2}$$

$$= 4/3 \text{ to } 5/3$$

$$dS = 0 \quad \Rightarrow \quad \frac{dP}{P} - \Gamma_1 \frac{d\rho}{\rho} = 0, \quad \text{Ledoux}$$

$$\frac{dP}{P} + \frac{\Gamma_2}{1 - \Gamma_2} \frac{dT}{T} = 0, \quad \text{Schwarzschild}$$

The latter is most frequently found in textbooks:

$$\frac{dP}{P} + \frac{\Gamma_2}{1-\Gamma_2} \frac{dT}{T} = 0$$

$$\left(\frac{dT}{dr} \right)_{rad} > \left(\frac{dT}{dr} \right)_{ad} = \left(1 - \frac{1}{\Gamma_2} \right) \frac{T}{P} \frac{dP}{dr}$$

implies convection
(Clayton 3-276)

$$-\frac{3}{4ac} \frac{\kappa\rho}{T^3} \frac{L(r)}{4\pi r^2} > \left(1 - \frac{1}{\Gamma_2} \right) \frac{T}{P} \frac{dP}{dr} \quad \frac{dP}{dr} = -\frac{GM(r)\rho}{r^2}$$

$$\Rightarrow L_{crit} = \frac{16\pi acG}{3\kappa} \left(1 - \frac{1}{\Gamma_2} \right) \frac{T^4}{P} M(r)$$

$$= \text{for ideal gas } 1.22 \times 10^{-18} \frac{\mu T^3}{\kappa\rho} M(r) \text{ erg/s}$$

$$\left. \vphantom{\frac{16\pi acG}{3\kappa}} \right\} P = \frac{\rho N_A k T}{\mu}$$

This is the Schwarzschild criterion

But, in fact, the criterion for convection can be written as either $A > 0$ or $B > 0$ where:

$$A = \frac{1}{\Gamma_1 P} \frac{dP}{dr} - \frac{1}{\rho} \frac{d\rho}{dr} \quad \text{LeDoux}$$

nb. each term is negative

$$B = \frac{\Gamma_2 - 1}{\Gamma_2} \frac{1}{P} \frac{dP}{dr} - \frac{1}{T} \frac{dT}{dr} \quad \text{Schwartzschild}$$

It can be shown for a mixture of ideal gas and radiation that

for $\nabla \equiv \frac{d \ln T}{d \ln P}$ $\nabla_L =$ threshold for Ledoux convection

$$\nabla_L = \nabla_S + \frac{\beta}{4 - 3\beta} \nabla_\mu \quad (\text{Langer et al 1983, 1985; Sakashita and Hayashi 1961;}$$

Kippenhan and Weigert - textbook - 6.12)

where $\nabla_\mu = \frac{d \ln \mu}{d \ln P}$ $\nabla_S = \left(\frac{d \ln T}{d \ln P} \right)_{ad}$ $\nabla_{rad} < \nabla_S, \nabla_L$ for stability

The two conditions are equivalent for constant composition, but otherwise Ledoux convection is more difficult.

Caveat:

$$\nabla_L = \nabla_S + \frac{\beta}{4 - 3\beta} \nabla_\mu$$

This is an approximation that is valid only for a mixture of ideal gas and radiation pressure. The general relation is more complicated if the gas is degenerate or includes pairs.

See Kippenhahn and Weigert and especially Heger, Woosley, and Spruit (ApJ, 626, 350 (2005) Appendix A) for a general treatment and for what is implemented in Kepler.

Semiconvection is the term applied to the slow mixing that goes on in a region that is stable by the strict Ledoux criterion but unstable by the Schwarzschild criterion.

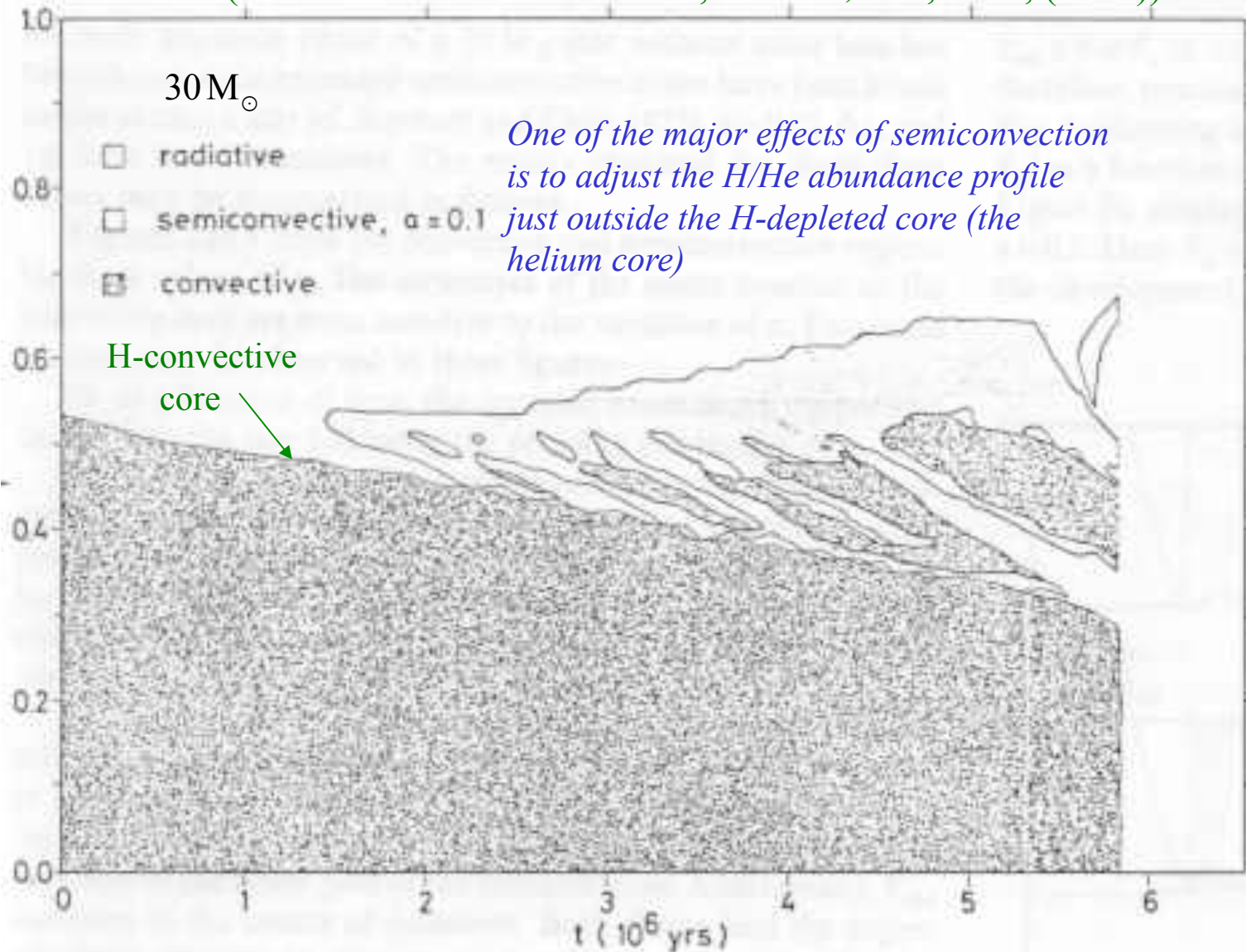
Generally it is thought that this process does not contribute appreciably to energy transport (which is then by radiative diffusion in semiconvective zones), but it does slowly mix the composition. Its efficiency can be measured by a diffusion coefficient that determines how rapidly this mixing occurs.

Many papers have been written both regarding the effects of semiconvection on stellar evolution and the estimation of this diffusion coefficient.

There are three places it is known to have potentially large effects:

- Following hydrogen burning just outside the helium core
- During helium burning to determine the size of the C-O core
- During silicon burning

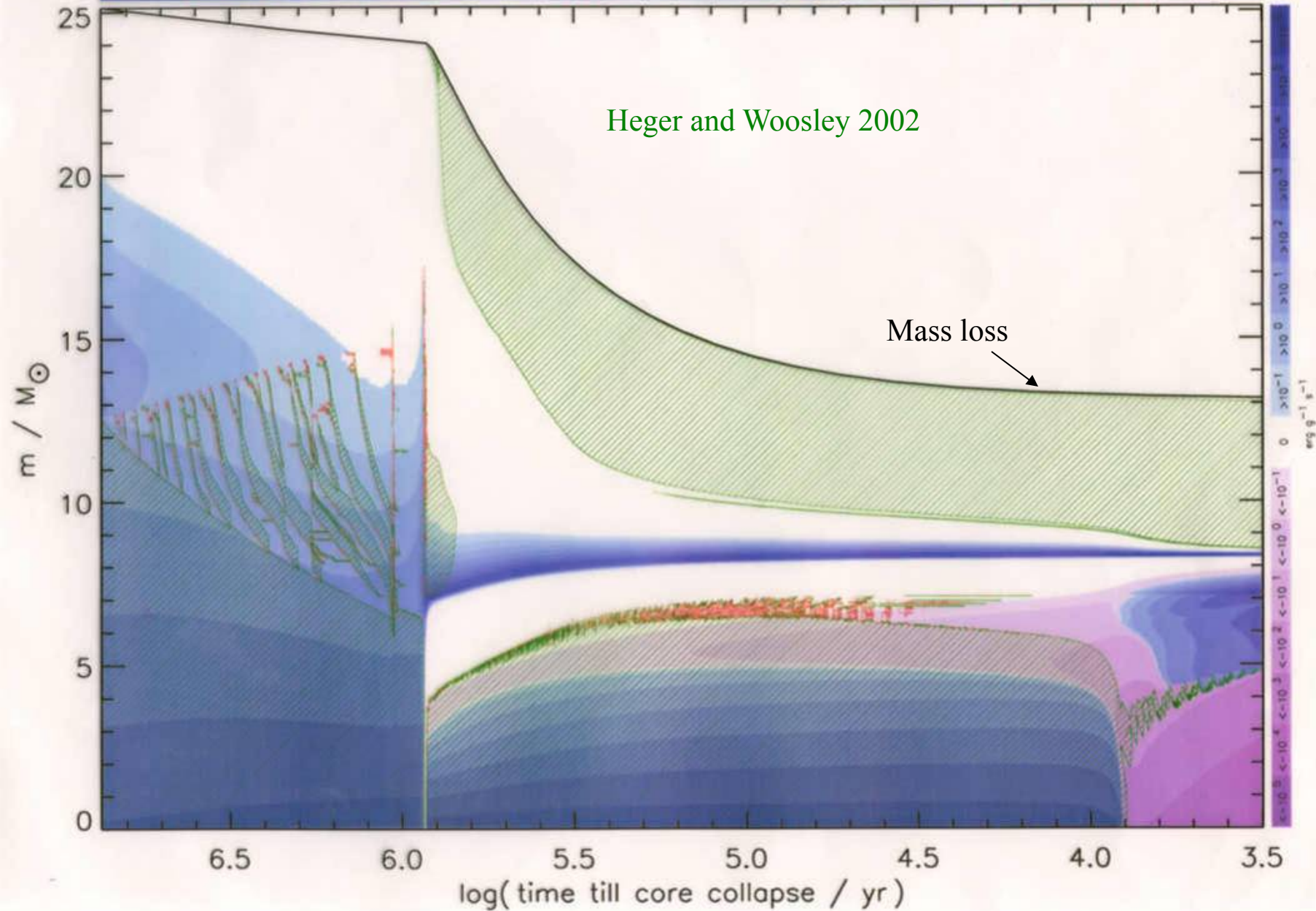
Langer, El Eid, and Fricke, *A&A*, **145**, 179, (1985)
(see also Grossman and Taam, *MNRAS*, **283**, 1165, (1996))



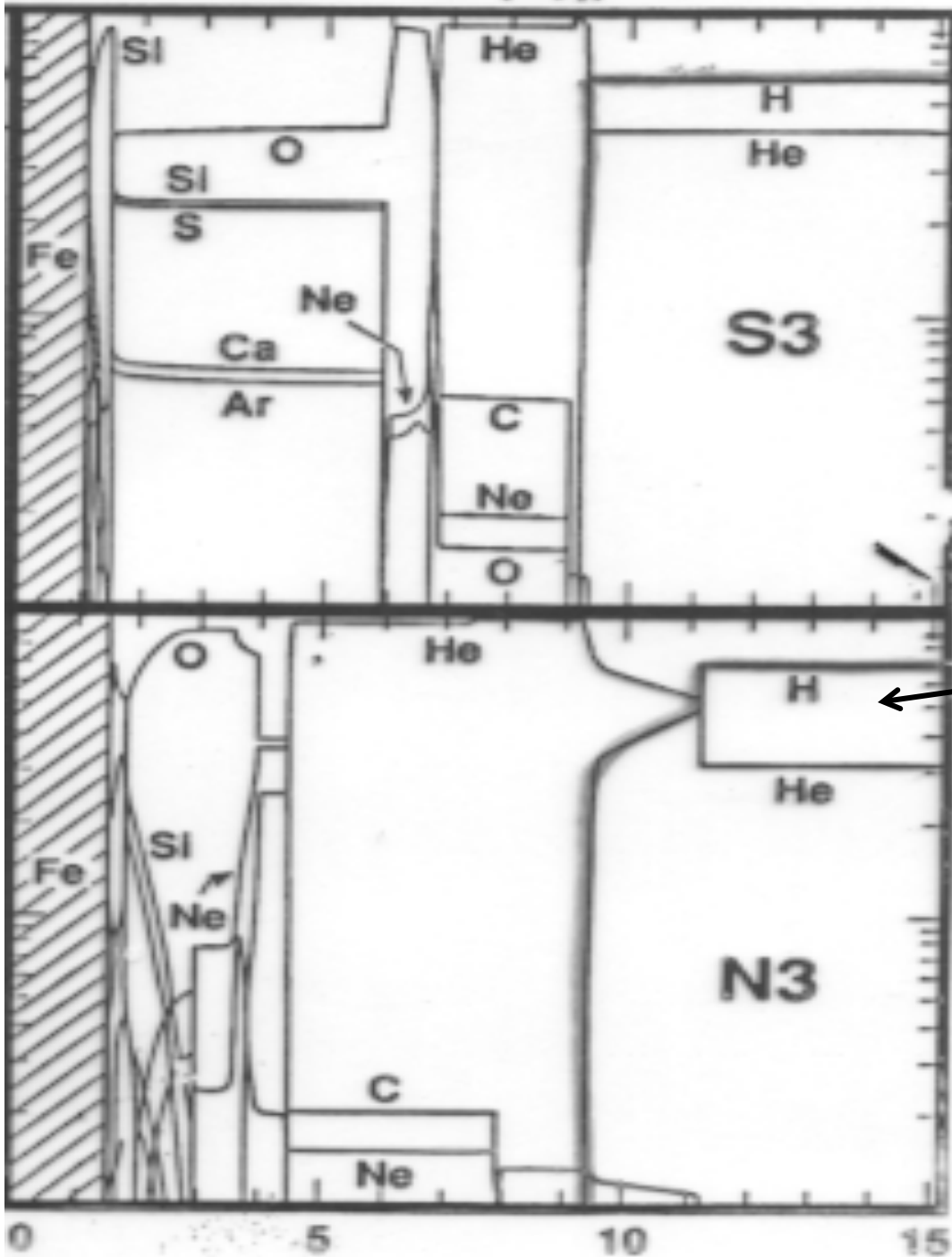
models

Heger and Woosley 2002

Mass loss



Woosley and
Weaver (1990)



$$D_{semi} \sim 0.1 D_{rad}$$

surface convection
zone

$$D_{semi} \sim 10^{-4} D_{rad}$$

- Shallower convection in H envelope
- Smaller CO core

For Langer et al., $\alpha \sim 0.1$ (their favored value) corresponds to $D_{\text{semi}} \sim 10^{-3} D_{\text{rad}}$, though there is not a real linear proportionality in their theory. The default in Kepler is $D_{\text{semi}} = 0.1 D_{\text{rad}}$.

By affecting the hydrogen abundance just outside the helium core, which in turn affects energy generation from hydrogen shell burning and the location of the associated entropy jump, semiconvection affects the envelope structure (red or blue) during helium burning. The two solutions are very narrowly separated and giant stars often spend appreciable time as both. It is very difficult to get a SN 1987A progenitor to be a BSG with Schwarzschild convection though it does predict longer residency as a BSG on the way to the red. **Pure Ledoux mixing gives many more red supergiants.** Too many.

A critical test is predicting the observed ratio of blue supergiants to red supergiants. This ratio is observed to increase rapidly with metallicity (the LMC and SMC have a smaller proportion of BSGs than the solar neighborhood).

Semiconvection alone, without rotational mixing, appears unable to explain both the absolute value of the ratio and its variation with Z (Langer & Maeder, *A&A*, **295**, 685, (1995)). LeDoux gives answer at low Z but fails at high Z . Something in between L and S favored overall, with rotational mixing included as well.

SN = solar neighborhood

Table 1. The B/R ratio in galaxies. Unless specified B means O, B and A stars

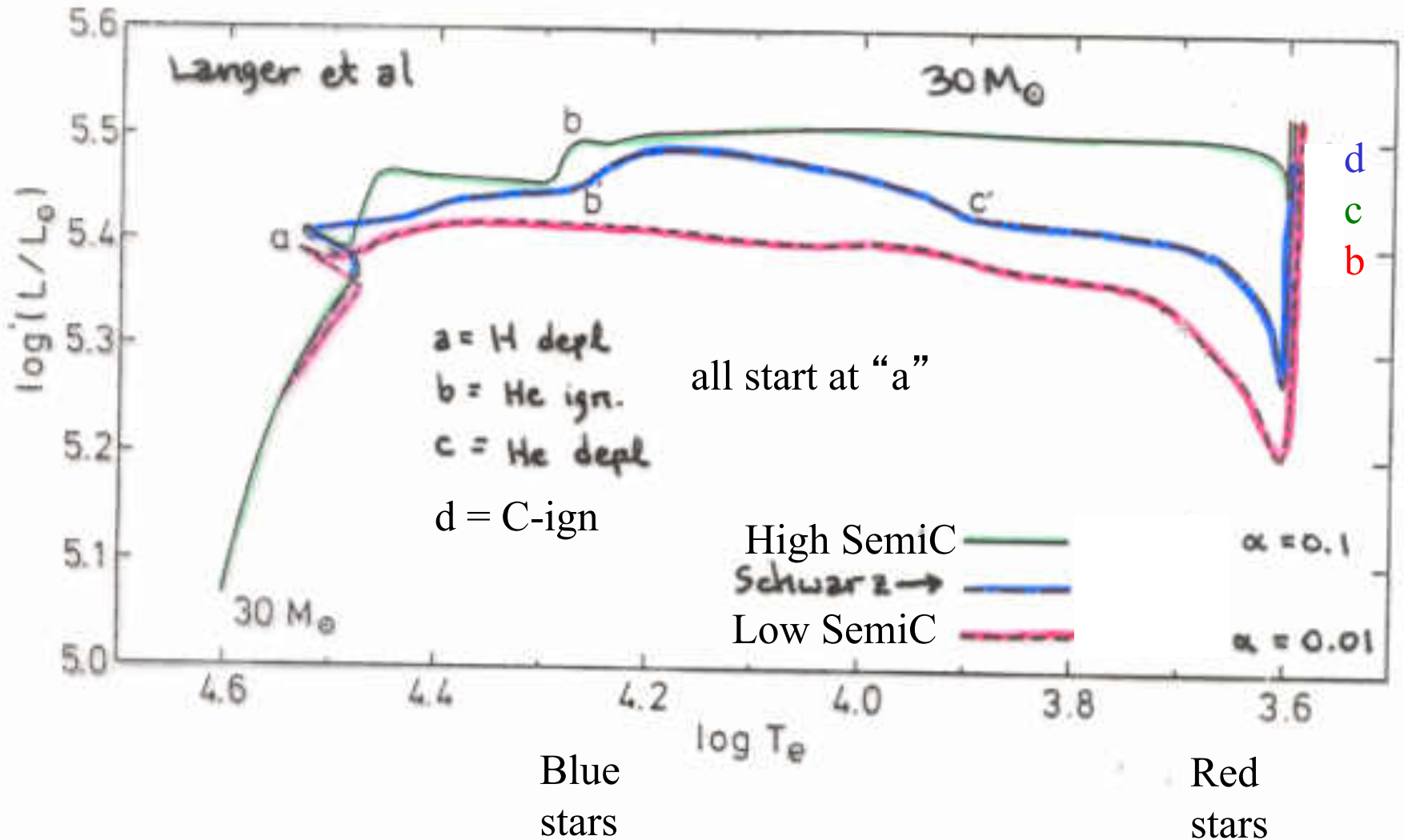
Z		SMC	LMC	outer MW	SN	inner MW
		.002	.006	.013	.02	.03
Stars,	$M_{bol} < -7^m 5^\dagger$	4	10	14	28	48:
Associations,	$M_{bol} < -7^m 5^\dagger$	4	10	14	30	89:
Clusters,	$M_V < -2^m 5^\ddagger$	2.5	6.7	7.7		20
counting only B supergiants						
NGC 330		0.5 ... 0.8				
Young clusters					3.6	

† Humphreys & McElroy (1984)

‡ Meylan & Maeder (1982)

Using Schwatzschild works for the galaxy but predicts B/R should increase at lower Z (weaker H shell), in contradiction with observations. Ledoux gives the low metallicity values OK but predicts too few BSG for the higher metallicity regions.

More semi-convection implies more BSG's
Less semi-convection implies more RSG's



Theory of semiconvection:

Kato – *PASJ*, **18**, 374, (1966) – an overstable oscillation at a sharp interface

Spruit – *A&A*, **253**, 131 (1992) – layer formation, double diffusive process. Relatively inefficient.

Merryfield – *ApJ*, **444**, 318 (1995) – 2D numerical simulation. Layers unstable. Mixing may be efficient.

Biello – PhD thesis, 2001, U. Chicago – 2D numerical simulation. Mixing relatively efficient.

Pascale Garaud, Justin Brown – in progress

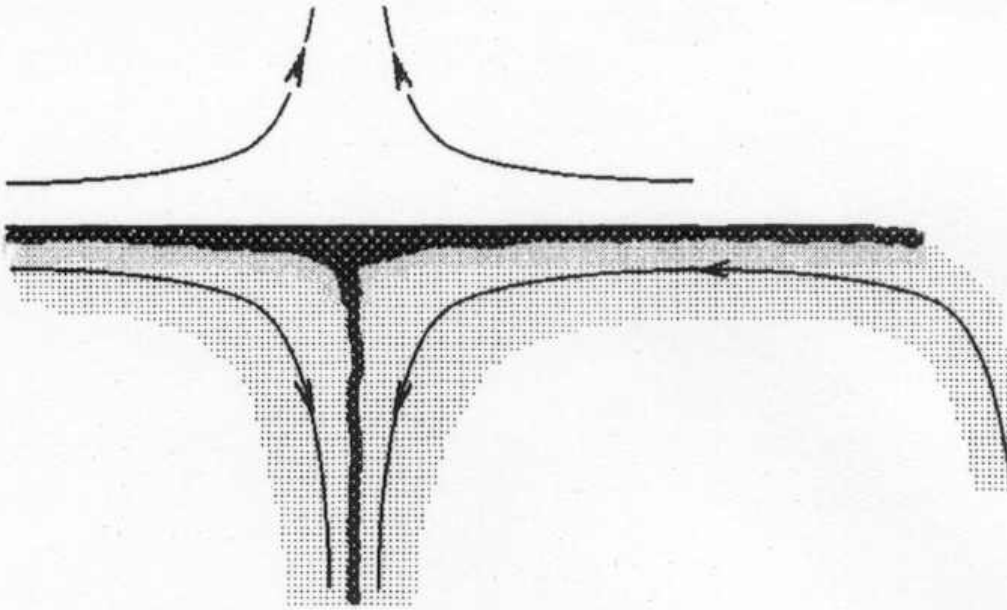


Fig. 2. Thermal (light shading) and solute (heavy shading) boundary layers at a diffusive interface. The solute boundary layer is much thinner than the thermal boundary layer due to the lower diffusivity. Descending and ascending plumes carry heat and solute away from the interface

Spruit (1992)

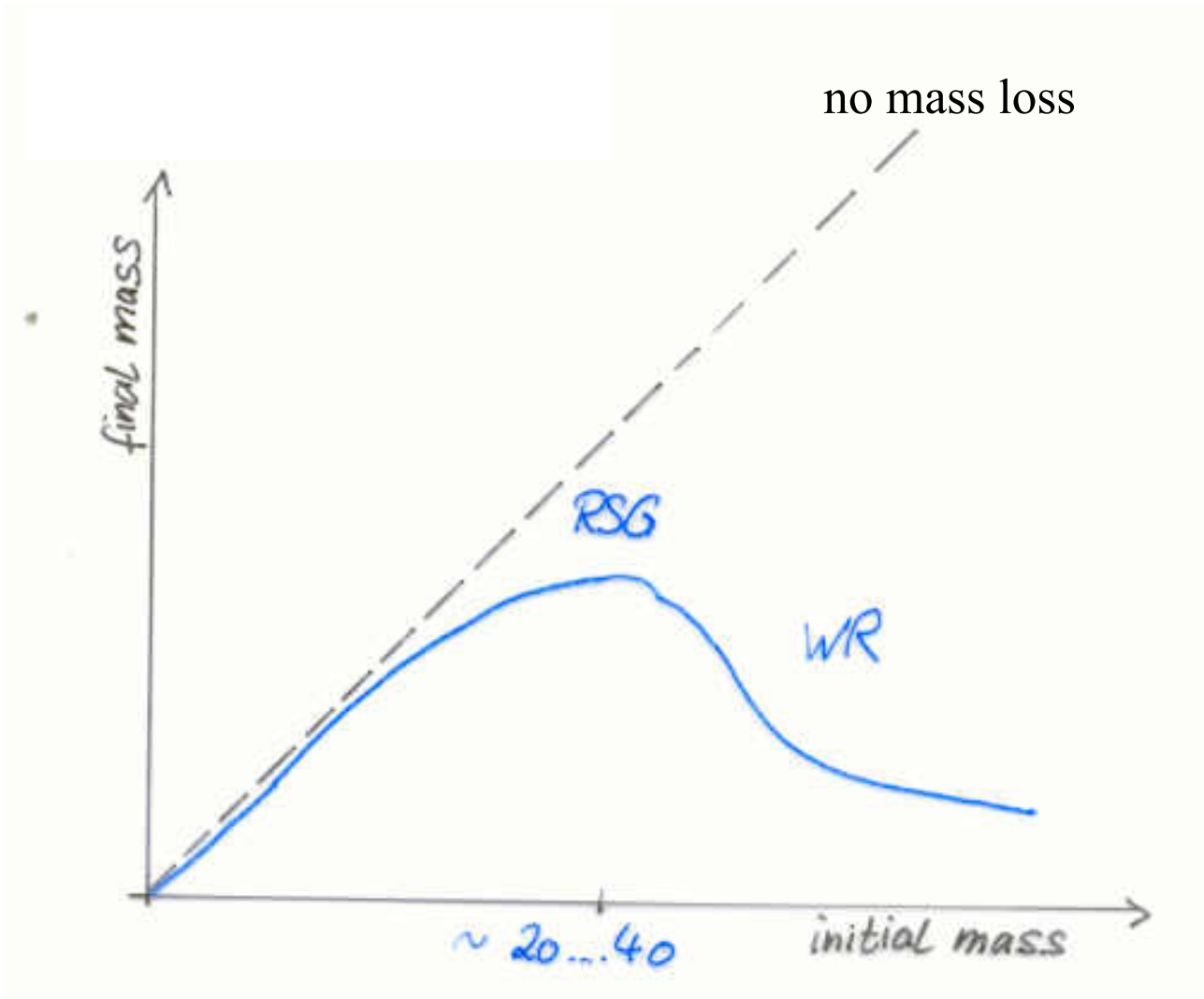
Convective cells form bounded by thin layers where the composition change is expressed almost discontinuously.

The diffusion coefficient is approximately the harmonic mean of the radiative diffusion coefficient and a much smaller ionic diffusion coefficient

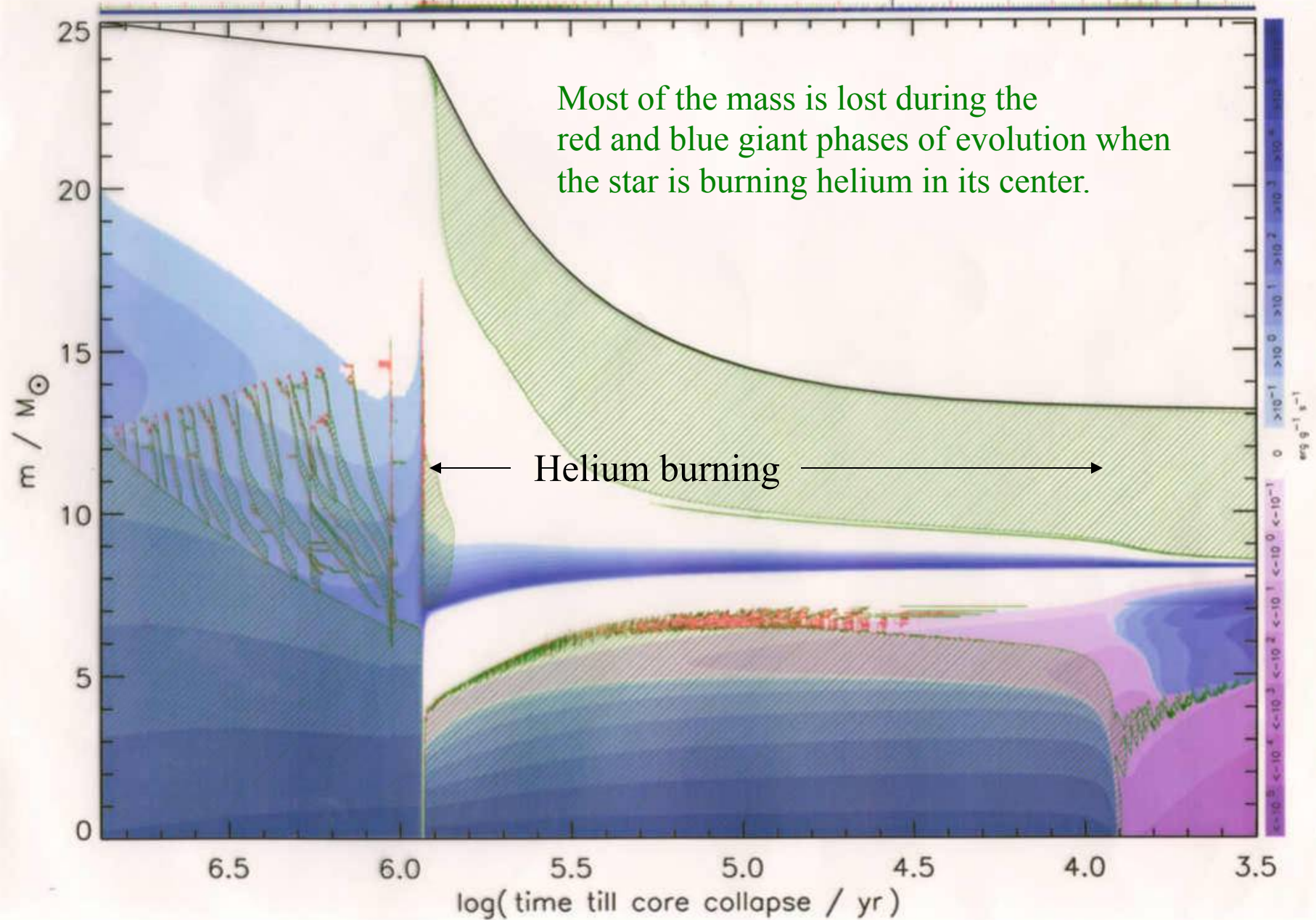
$$\kappa_{s \text{ eff}} = (\kappa_s \kappa_t)^{1/2} \left(\frac{4}{\beta} - 3 \right) \frac{\nabla_r - \nabla_a}{\nabla_\mu} \min \left[1, \frac{1}{2} q^{3/2} \right].$$

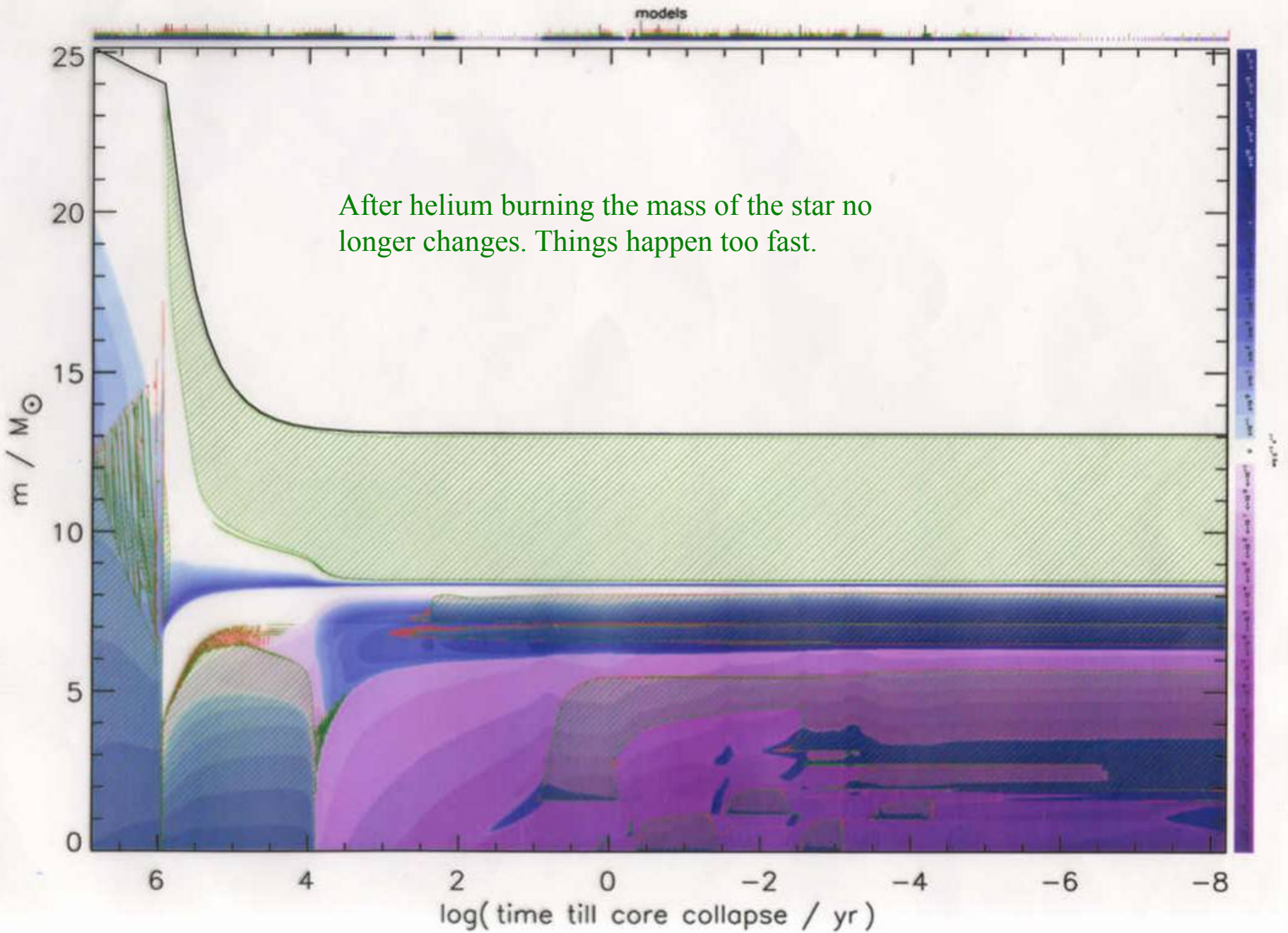
q is a correction factor that applies when the convective turnover is short relative to the diffusion time. Spruit argues that q typically < 1 .

Mass Loss



models





Mass loss – general features

See Chiosi & Maeder, *ARAA*, **24**, 329 (1986) and Kudritzki and Puls, *ARAA*, **38**, 613 (2000) for reviews. The latter is for hot stars.

For how mass loss rates are measured see Dupree, *ARAA*, **24**, 377 (1986) – high resolution spectroscopy in IR, optical and uv; also radio measurements

For a review of the physics of mass loss see Castor in *Physical Processes in Red Giants*, ed. Iben and Renzini, Dordrecht: Reidel. See also Castor, Abott, & Klein, *ApJ*, **195**, 157 (1975)

In massive stars, mass loss is chiefly a consequence of radiation pressure on atoms (main sequence) and grains (giant stars). In quite massive stars, shocks, turbulence, and the approaching Eddington limit may be important.

Mass Loss – Implications in Massive Stars

- 1) May reveal interior abundances as surface is peeled off of the star. E.g., CN processing, s-process, He, etc.
- 2) Structurally, the helium and heavy element core – once its mass has been determined is not terribly sensitive to the presence of a RSG envelope. If the entire envelope is lost however, the star enters a phase of rapid Wolf-Rayet mass loss that does greatly affect everything – the explosion, light curve, nucleosynthesis and remnant properties. A massive hydrogen envelope may also make the star more difficult to explode because of fall back. BSG envelopes may also exert substantial pressure.
- 3) Mass loss sets an upper bound to the luminosity of red supergiants. This limit is metallicity dependent. For solar metallicity, the maximum mass star that dies with a hydrogen envelope attached is about 35 solar masses.
- 4) Mass loss – either in a binary or a strong wind – may be necessary to understand the relatively small mass of Type Ib supernova progenitors. In any case it is necessary to remove the envelope and make them Type I.

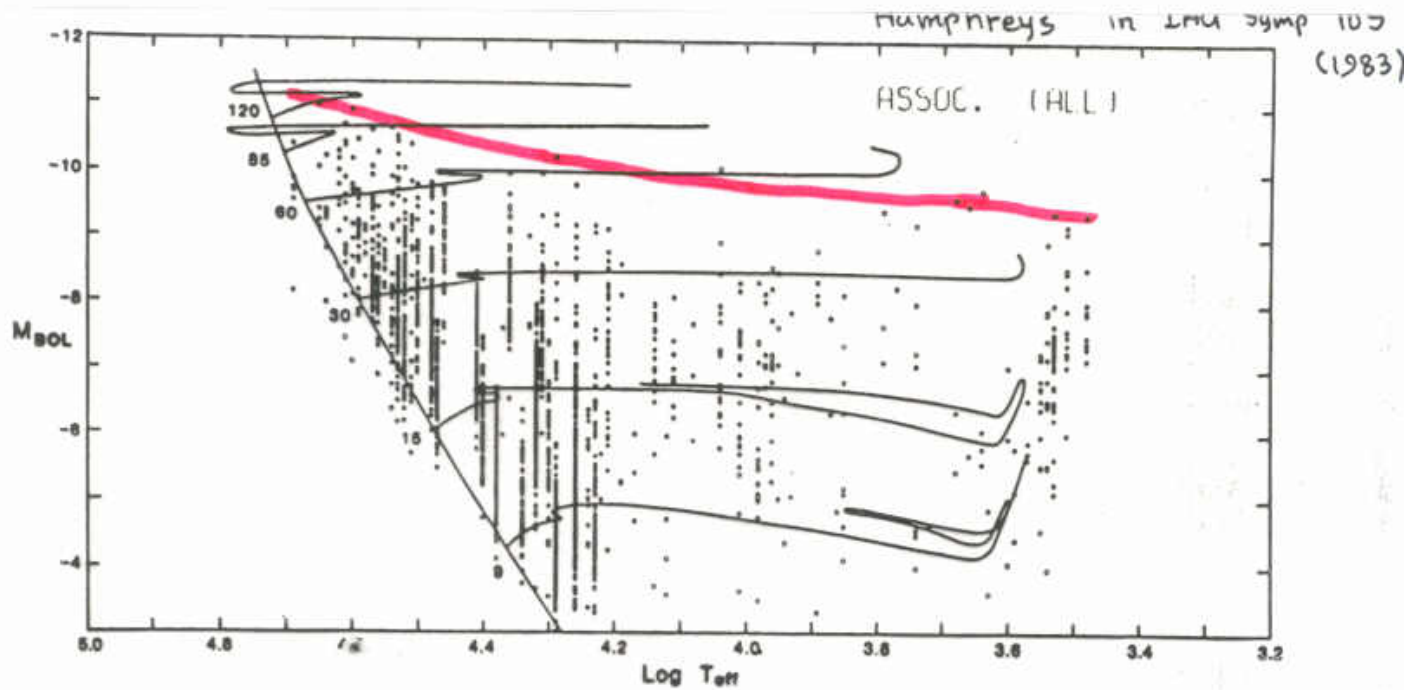


Figure 1 - The HR diagram, M_{BOL} vs. $\log T_{\text{eff}}$, for O-type stars, supergiants, and less luminous early-type stars in 91 stellar associations and clusters in the solar region of our Galaxy.

Humphreys, R. M., & Davidson, K. 1979, ApJ, 232, 40
No RSG's brighter than $M = -9$.

- 5) Determines the lightest star that can become a supernova (and the heaviest white dwarf). Electron capture SNe? SNe I.5?
- 6) The nucleosynthesis ejected in the winds of stars can be important – especially WR-star winds.
- 7) In order to make gamma-ray bursts, the hydrogen envelope must be lost, but the Wolf-Rayet wind must be mild to preserve angular momentum.
- 8) The winds of presupernova and preGRB stars influence their radio luminosities
- 9) Mass loss can influence whether the presupernova star is a red or blue supergiant.
- 10) The calculation of mass loss rates from theory is an important laboratory test ground for radiation hydrodynamics.

Especially uncertain are the mass loss rates for “Luminous Blue Variable” stars (LBV). These stars are quite massive, probably over 35 solar masses, and represent a transition from the main sequence to the Wolf-Rayet stage that does not necessarily pass through the red giant stage.

Such massive stars are approaching the Eddington limit and have loosely bound envelopes. Mass loss may be episodic with up to several solar masses coming off at once (η -Carina).

See Humphreys and Davidson, PASP, 106, 1025, (1994)

Humphreys and Davidson (1994)

In a typical LBV eruption, the star's photosphere expands and the apparent temperature decreases to near 8000 K. During these normal eruptions the bolometric luminosity remains constant, as typified by S Doradus, AG Carinae, and R 127. A few LBV's, specifically Eta Carinae, P Cygni, V12 in NGC 2403, and SN 1961V, have giant eruptions in which the total luminosity actually increases by more than one or two magnitudes. The star may expel as much as a solar mass or more with a total luminous output rivaling a supernova. The classical LBVs have luminosities greater than M_{bol} approximately equal to -9.6 mag, suggesting initial mass greater than 50 solar mass. These stars have very likely not been red supergiants as there are no evolved cool stars of comparable luminosity.

Typical implementation of mass loss (except for WR stars):

Nieuwenhuijzen and de Jager, *A&A*, **231**, 134, (1990)

$$\dot{M} = 9.63 \times 10^{-15} \left(\frac{L}{L_{\odot}} \right)^{1.42} \left(\frac{M}{M_{\odot}} \right)^{0.16} \left(\frac{R}{R_{\odot}} \right)^{0.81} M_{\odot} \text{ yr}^{-1}$$

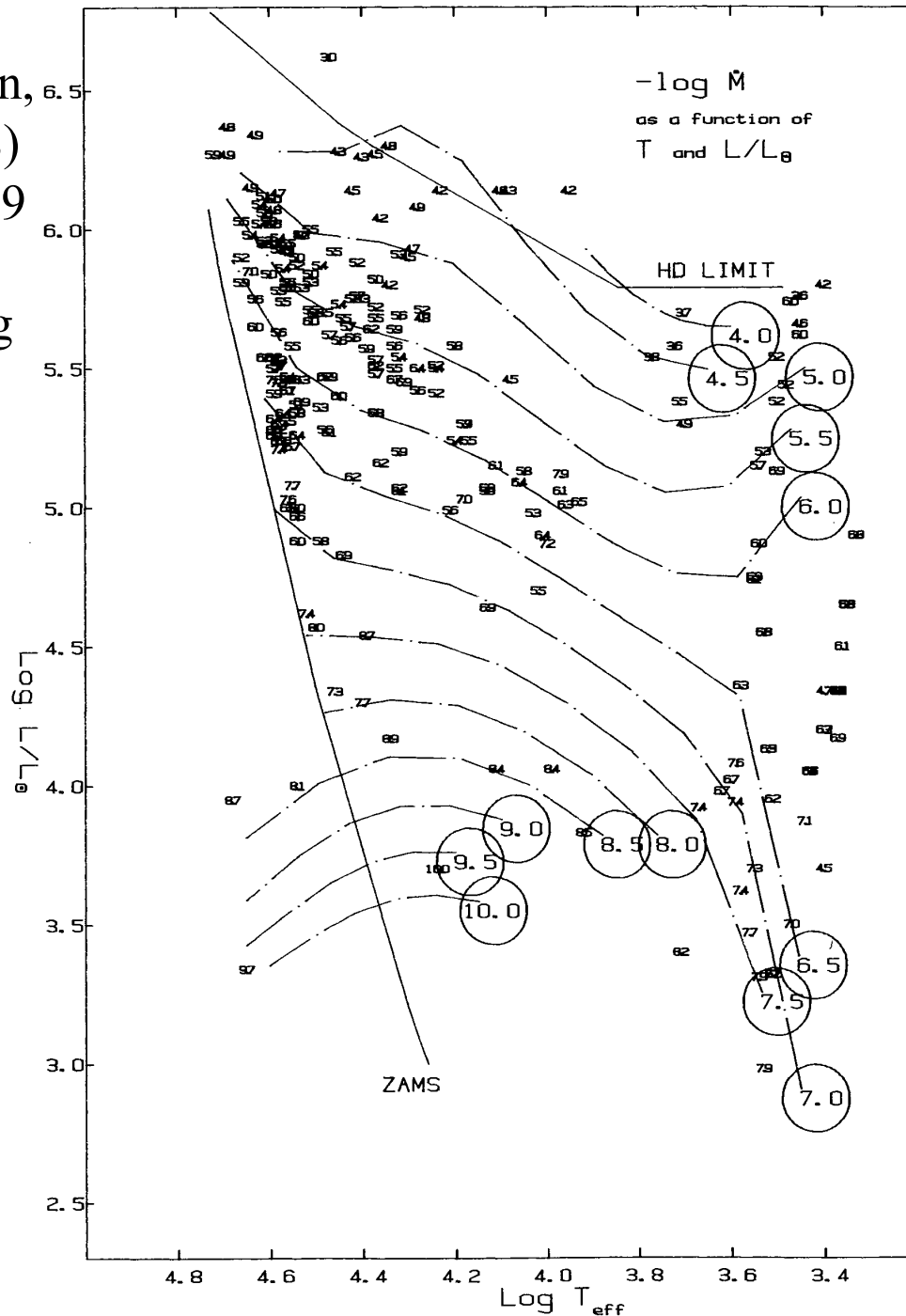
across the entire HR-diagram. This is multiplied by a factor to account for the metallicity-dependence of mass loss.

Studies by of O and B stars including B-supergiants, by Vink et al, *A&A*, **369**, 574, (2001), indicate a metallicity sensitivity with scaling approximately as $Z^{0.65}$.

Kudritzski, *ApJ*, **577**, 389 (2002) in a theoretical treatment of stellar winds (non-LTE, 2 million lines). Mass loss rate approximately proportional to $\sim Z^{1/2}$ down to $Z = 0.0001$ times solar.

de Jager, Nieuwenhuijzen,
and van der Hucht (1988)
Aston, Ap. Suppl., 72, 259

Circled numbers are $-\log$
base 10 of the mass loss
rate.



Wolf-Rayet stars – Langer, A&A, 220, 135, (1989)

$$\dot{M}_{\text{WR}} = (0.6 - 1.0) \times 10^{-7} \left(\frac{M_{\text{WR}}}{M_{\odot}} \right)^{2.5} M_{\odot} \text{ yr}^{-1}$$

Wellstein and Langer (1998) corrected this for Z-dependence and divided by 3 to correct for clumping is what we currently use.

$$\log(-\dot{M}_{\text{WR}} / M_{\odot} \text{ yr}^{-1}) = -11.95 + 1.5 \log(L / L_{\odot}) - 2.85 X_s$$

for $\log(L / L_{\odot}) \geq 4.5$

$$= -35.8 + 6.8 \log(L / L_{\odot})$$

for $\log(L / L_{\odot}) < 4.5$

Here X_s is the surface hydrogen mass fraction (WN stars) and the result should be multiplied by $1/3 (Z/Z\text{-solar})^{1/2}$.

Woosley, Langer, and Weaver, ApJ, 448, 315, (1995)

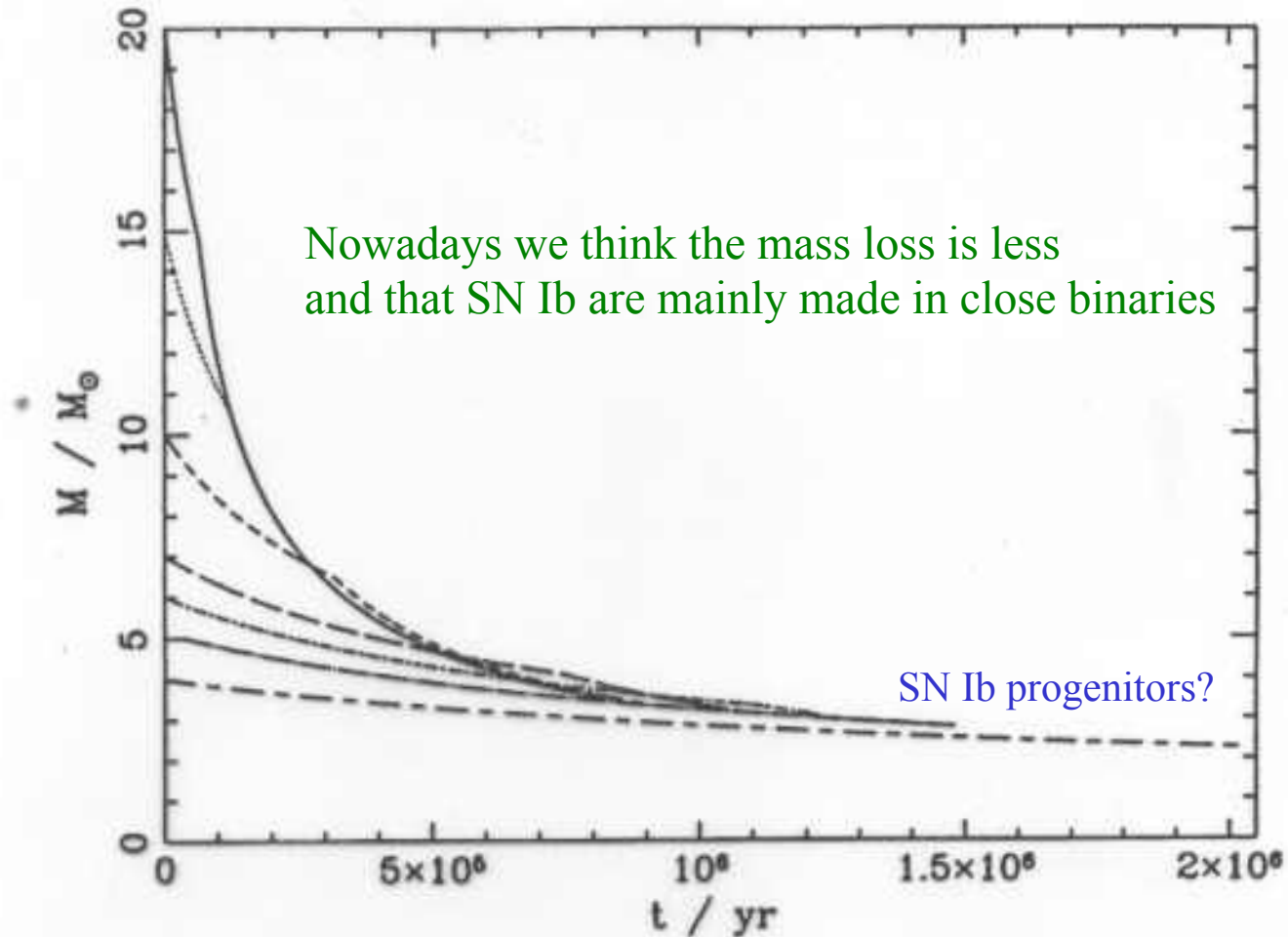
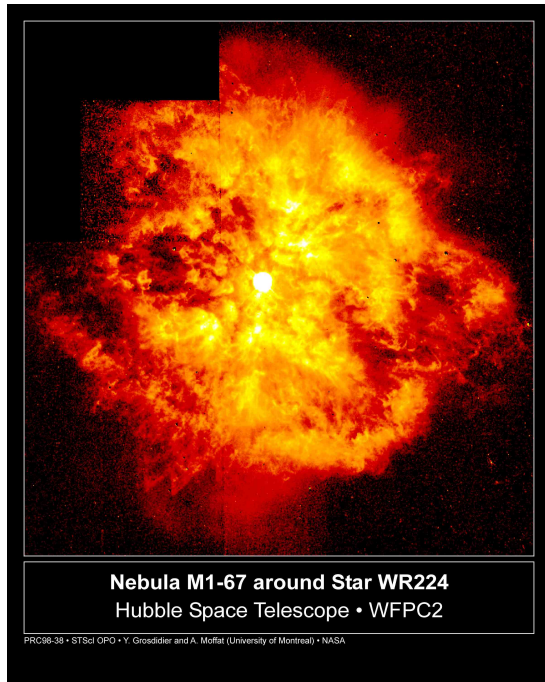


FIG. 1.—Total stellar mass as function of time for our sequences with initial masses of 20, 15, 10, 7, 6, 5, and 4 M_{\odot} . Mass convergence due to mass-dependent mass loss is clearly visible.

Wolf-Rayet stars (continued)



The Wolf-Rayet star WR224 is found in the nebula M1-67 which has a diameter of about 1000 AU

The wind is clearly very clump and filamentary.

Vink and DeKoter (2005)

$$\dot{M}_{WR} \propto Z^{0.86}$$

where Z is the initial metallicity (i.e., Fe) of the star, not the C,O made at its surface. This is true until such low metallicities that the mass loss rate is quite small. ***Crucial for GRBs**

with mass loss, the final mass of a star does not increase monotonically with its initial mass. (e.g., Schaller et al. A&A, (1992))

Initial Mass	Final Mass		
	Z=0.02 (Sch92)	Z=0.015 (Woo07)	Z=0.001 (Sch92)
7	6.8		6.98
9	8.6		8.96
12	11.5	10.9	11.92
15	13.6	12.8	14.85
20	16.5	15.9	19.4
25	15.6	15.8	24.5
40	8.12	15.3	38.3
60	7.83	7.29	46.8
85	8.98	6.37	61.8
120	7.62	6.00	81.1

He- core
↑
uncovered
↓

Because of the assumed dependence of mass loss on metallicity, stars of lower metallicity die with a higher mass. This has consequences for both the explosion and the nucleosynthesis.

Final masses (Schaller et al (1992))

	standard	$\dot{M} * 2$
12	11.52	
15	13.59	
25	15.58	
20	16.52	13.95
25	15.58	11.30
40	8.11	3.57
60	7.83	4.96
85	8.97	3.49
120	7.61	2.35

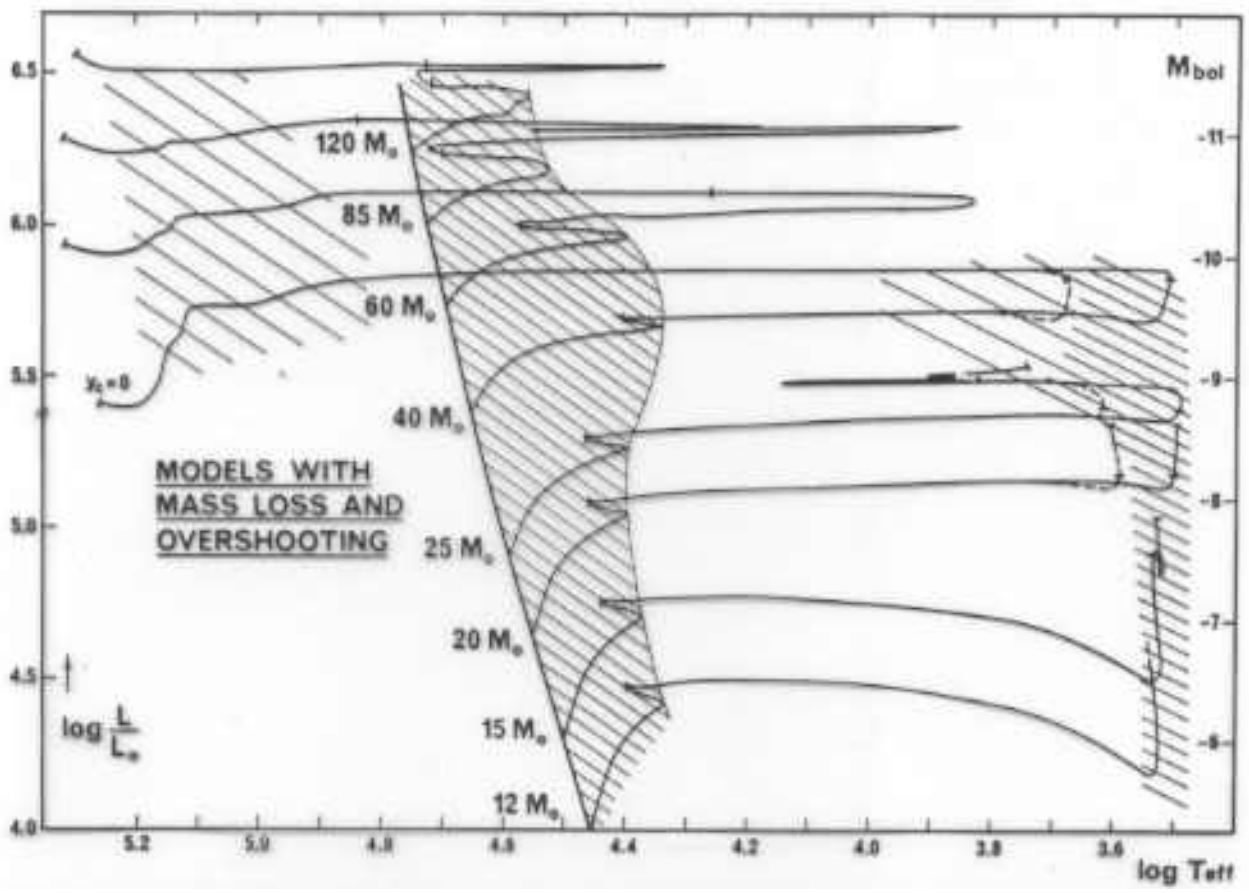
Characteristics of Wolf-Rayet Stars

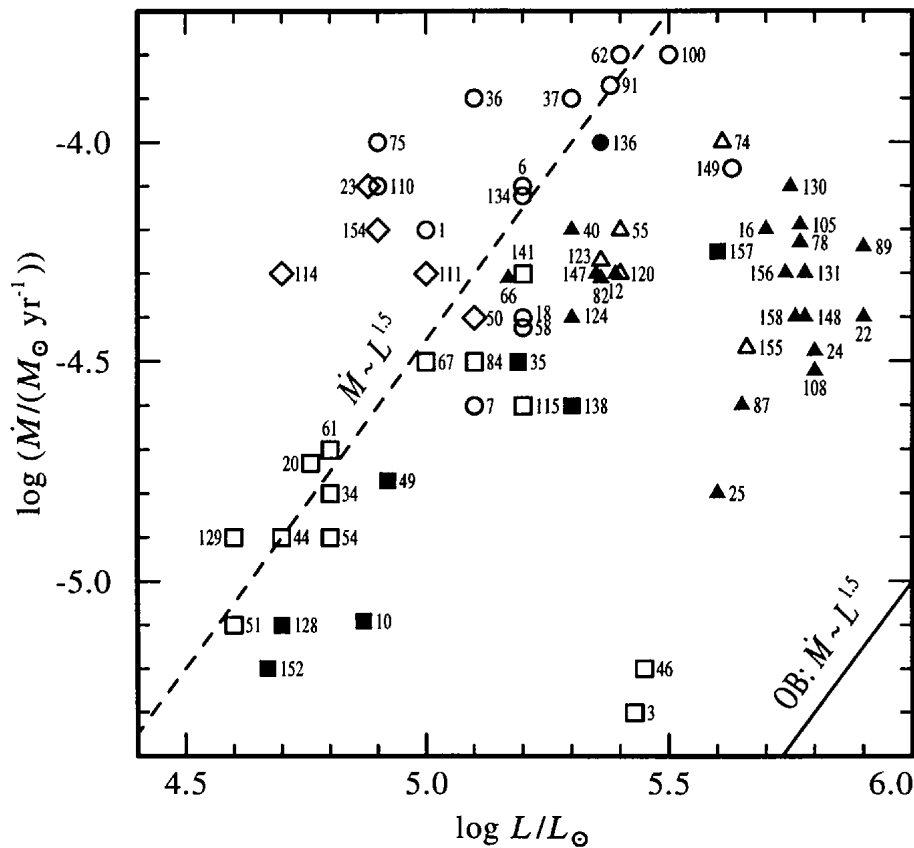
- high luminosities
- strong, broad emission lines
- dense, optically thick stellar winds
wind accelerated by multiple scattering of photons
- high mass loss rates
typically $\dot{M} \approx 4 \cdot 10^{-5} M_{\odot} \text{ yr}^{-1}$
- high terminal wind velocities
(1 000 ... 2 500) km s^{-1}

- "photospheric" temperatures
(20 000 ... 40 000) K
- masses (5 ... 30) M_{\odot} common but a wide variation is seen
- hydrogen poor (WNL) or completely absent
- products of hydrogen and helium burning appear at the surface
↳ mixing and/or loss of outer layers
- recent progress: WR wind is clumpy!
mass loss rates (as determined from fit to WR spectra) may be lower by a factor of 2 ... 4 than assumed before
(Hamann & Koesterke 1998, A&A 335, 1003)
- Rotation rates and masses not very well determined observationally except in a few cases (binaries)

Classification of Wolf-Rayet Stars

- "early" (hot; WxE) and "late" (cooler, WxL) types
- WN stars show helium lines (HeI, HeII) and lines of ionized nitrogen (NIII, NIV, NV)
- WC stars show lines of ionized carbon (CIII, CIV) and oxygen (OIV, OV, OVI)
- WC stars where oxygen lines dominate over carbon lines are also called WO stars.
- decreasing levels of ionization are denoted by decreasing arabic numbers
 - WNE = WN2...WN6
 - WNL = WN7...WN10
 - WCE = WC4...WC6
 - WCL = WC7...WC10
- WNE stars are subdivided in stars with strong (WNE-s) and weak (WNE-w) emission lines. WNE-s stars experience much higher mass loss rates than WNE-w stars.
(Schmutz, Hamann, Wessolowski 1989, A&A, 210, 236)
- WNL stars show some (up to 40%) hydrogen





Filled symbols mean detectable H. These have systematically lower loss rates.

Figure 2. Mass-loss rates of Galactic WR stars versus luminosity. The individual stars are labeled by their WR number. Triangles, squares and circles refer to WNL, WNE-w and WNE-s stars, respectively. Five WC stars with well-established data are also represented (diamonds). Filled and open symbols indicate whether hydrogen is detectable or absent, respectively. The dashed line gives a tentative fit to the mass-loss rates of *hydrogen-free* WN stars, while those WN stars *with hydrogen* lie to the lower-right of that relation. The corresponding relation for OB stars is indicated at the lower-right corner. (After Hamann *et al.* 1995a)

Masses?

Typical masses are around 16 to 18 M_{\odot} but the range is very great: from 3 M_{\odot} to 48 M_{\odot} or, in one case (WR 22*, HD 92740), 77 M_{\odot} . Masses of the O star in W-R+O binary systems range from 14 to 57 M_{\odot} , with a mean of 33 M_{\odot} (Cherepashchuk 1992, p. 123).

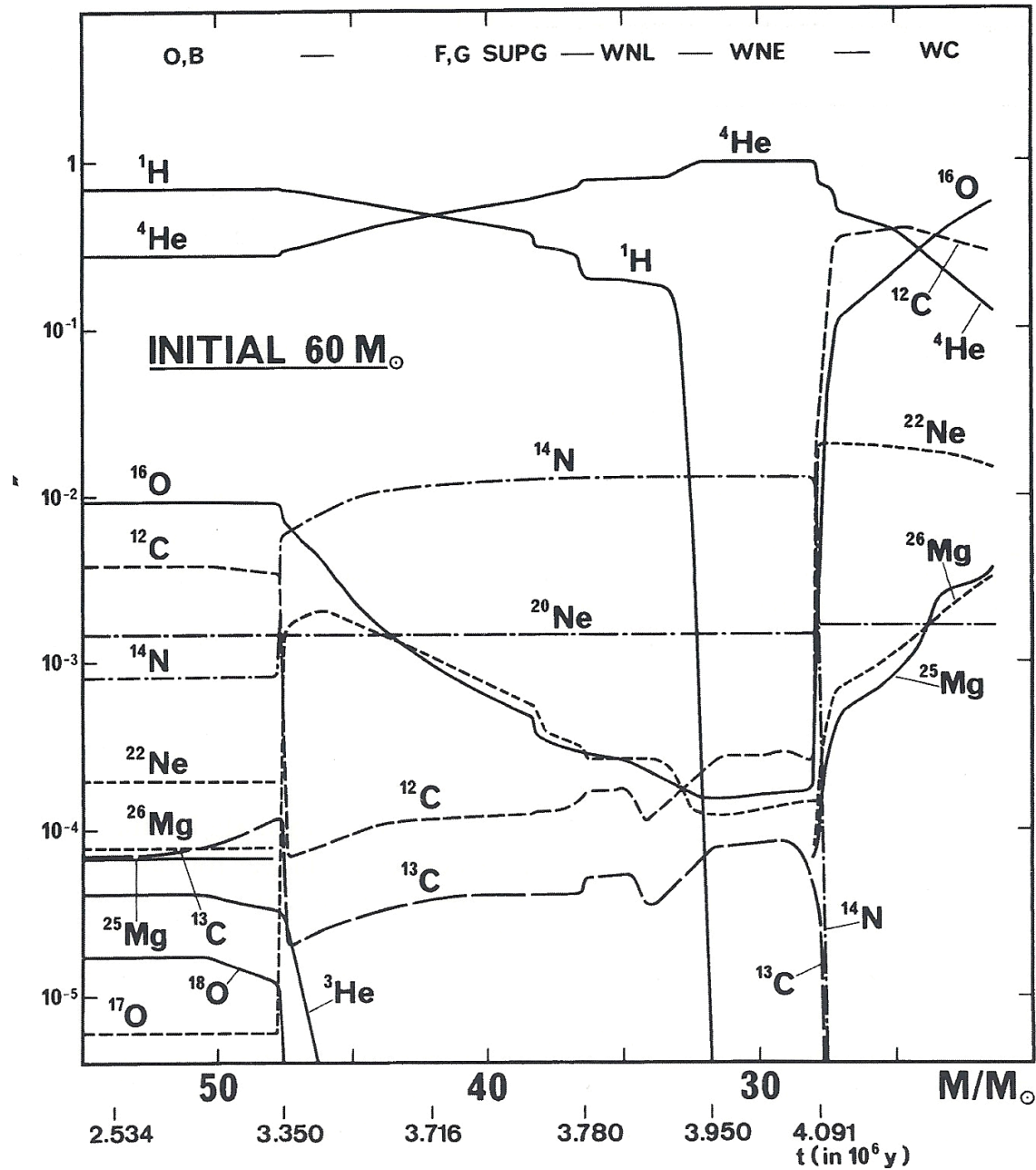
Cherepashchuk et al. (1992) in *Evolutionary Processes in Interacting Binary Stars*, IAU Proc. 151, p 123

*Some say WR 22 might be an Of star burning hydrogen

Mean mass 22 determinations - 15.6 - 18.4

Cherespashchuk, Highly Evolved Close Binary Stars Catalogue
Advances in A & A, vol 1, part 1, 1996

Maeder (1987)



Masses(actual): $\sim 8-25 M_{\odot}$ (up to $80 M_{\odot}$ for H-rich WR stars).
 Luminosities: $\sim 10^5-10^{6.5} L_{\odot}$.
 Eddington factor: ~ 0.7 to ~ 1.0 .
 T_{eff} : $\sim 3 \times 10^4$ to 1.5×10^5 K (Sect. 27.5.2).
 \dot{M} : $\sim 5 \times 10^{-6}$ to $10^{-4} M_{\odot} \text{ yr}^{-1}$.
 WN chemistry: H, He, N (products of CNO burning).
 WC chemistry: He, C, O, no H (products of He burning).

TENTATIVE FILIATIONS:

Always blue

$M > 90 M_{\odot}$: O – Of – WNL – (WNE) – WCL – WCE – SN (Hypernova ?)

$M > 60-90 M_{\odot}$: O – Of/WNL \leftrightarrow LBV – WNL(H poor) – WCL-E – SN (SNIIn?)

$M > 40-60 M_{\odot}$: O – BSG – LBV \leftrightarrow WNL – (WNE) – WCL-E – SN (SNIb)
 – WCL-E – WO – SN (SNIc)

Blue – red - blue

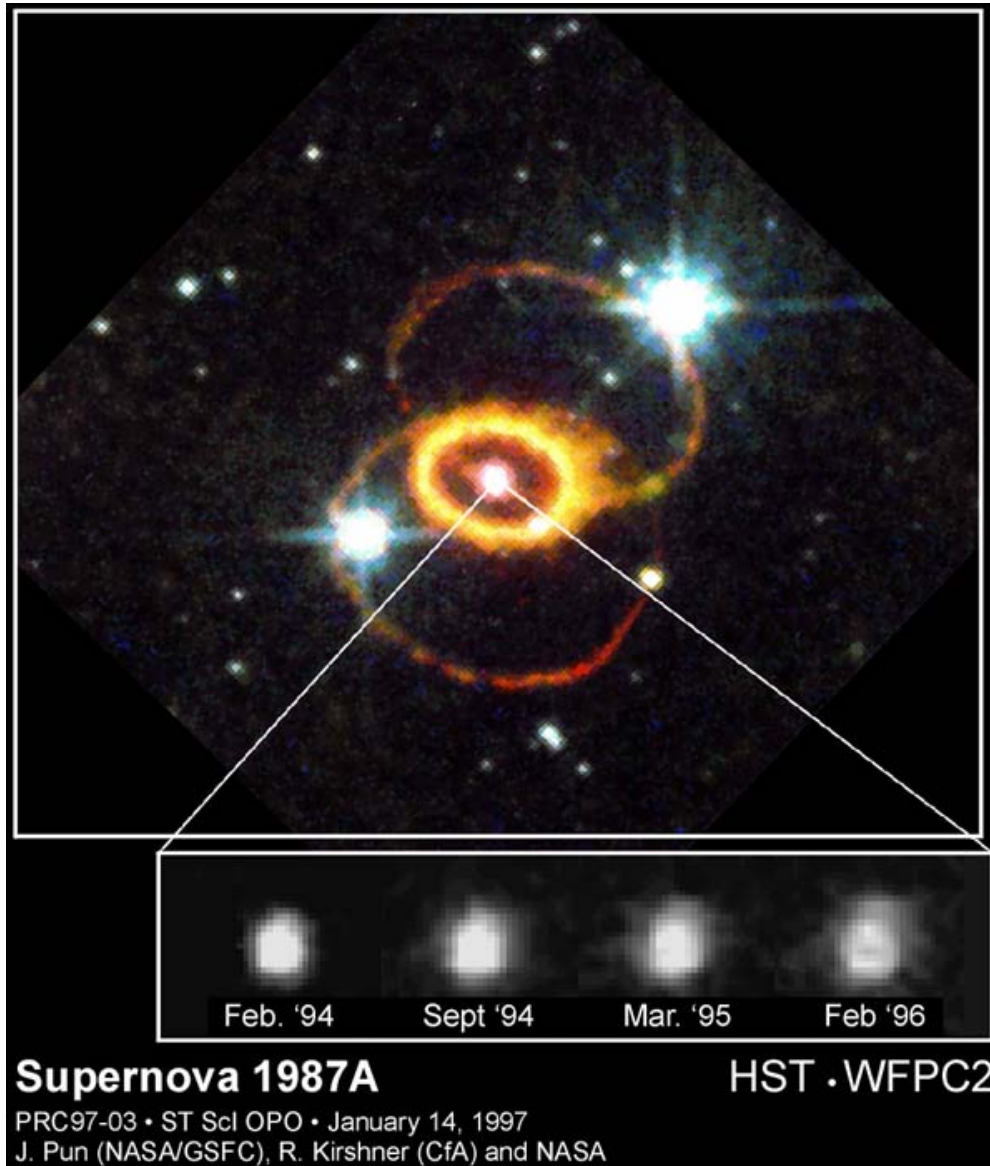
$M > 30-40 M_{\odot}$: O – BSG – RSG – WNE – WCE – SN (SNIb)
 OH/IR \leftrightarrow LBV ?

Blue – red

$M > 25-30 M_{\odot}$: O – (BSG) – RSG – BSG \leftrightarrow RSG SNIIIL
 BLUE LOOP

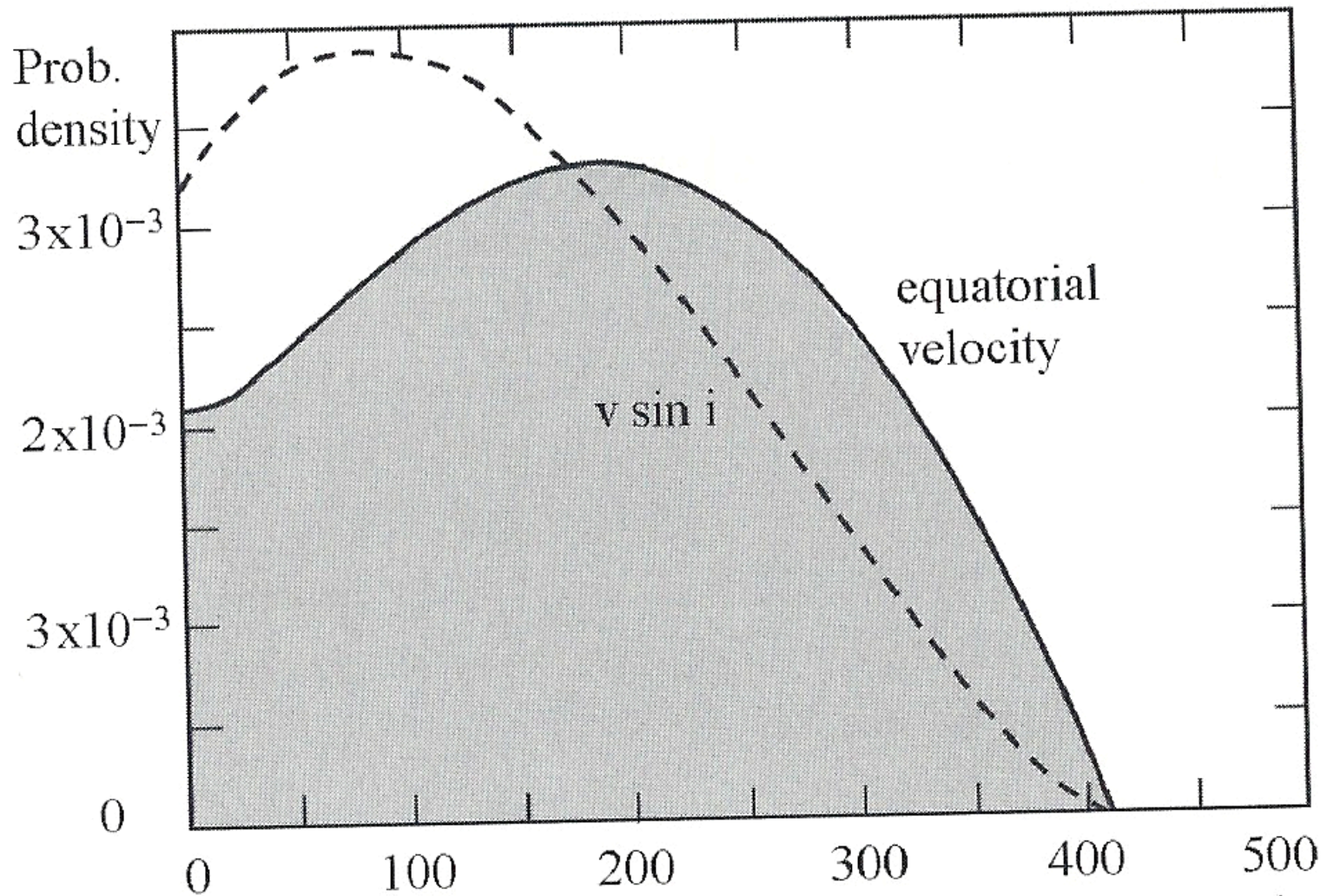
$M > 10-25 M_{\odot}$: O – RSG – (Cepheid loop for $M < 15 M_{\odot}$) – RSG – SN SNIIp

Rotation



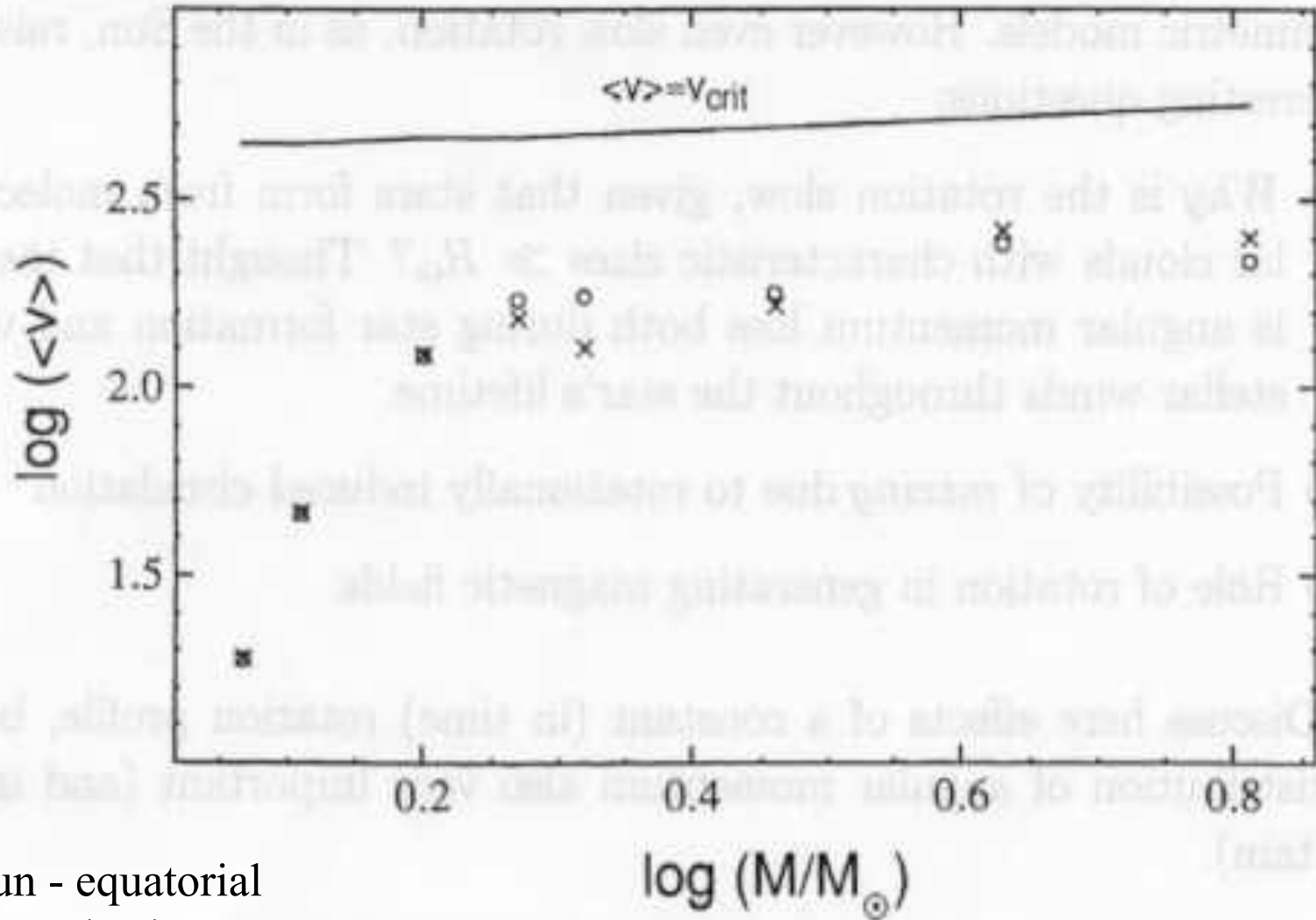
Blue
Supergiant
Sher 25
with a ring.





Huang and Gies (2006) for 495 main sequence stars of Type B8 to O9.5. Analysis includes variation of line strength with effective gravity over surface of deformed rotating star. See also Huang et al (ApJ, 722, 605, (2010)). Many stars near rotational shedding limit.

much more important than in low mass stars



Sun - equatorial
2 km/s

Eddington-Sweet Circulation

See Kippenhahn and Wiegert, Chapter 42, p 435ff for a discussion and mathematical derivation.

For a rotating star in which centrifugal forces are not negligible, the equipotentials where gravity, centrifugal force and pressure are balanced will no longer be spheres. A theorem, Von Zeipel's Theorem, can be proven that shows that for a generalized potential

$$\Psi = \Phi + V = \text{gravitational potential} - \int_0^s \omega^2 s \, ds \quad \omega^2 s \vec{e}_s = -\nabla V$$

$$\nabla P = -\rho \nabla \Psi$$

generalization of

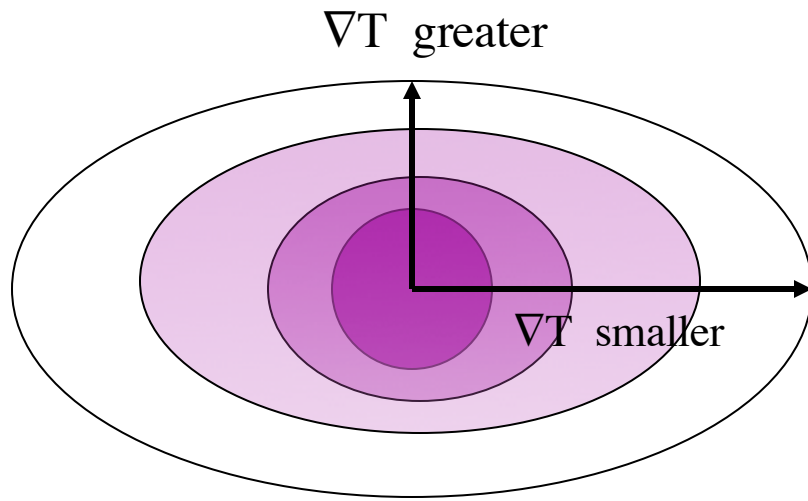
$$\frac{dP}{dr} = \frac{-GM\rho}{r^2}$$

centrifugal potential

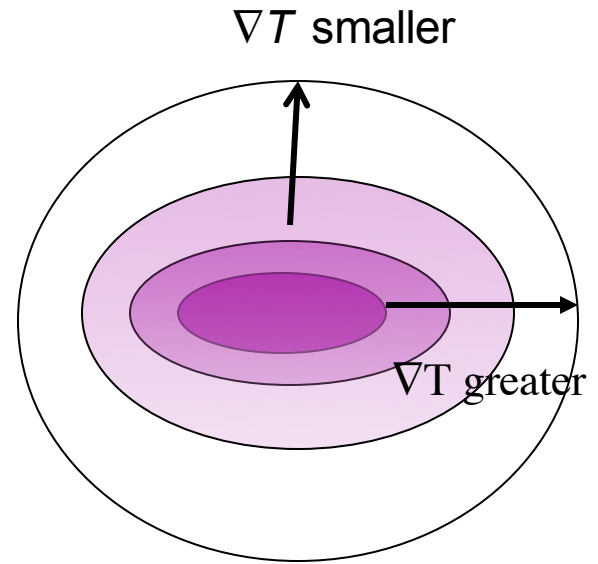
where s is the distance from the axis

Surfaces of constant Ψ , i.e., "equipotentials", will also be surfaces of constant pressure, temperature, density, and energy generation rate.

However, in this situation, the equipotentials will *not* be surfaces of constant heat flux because the temperature gradient normal to the surface will vary.

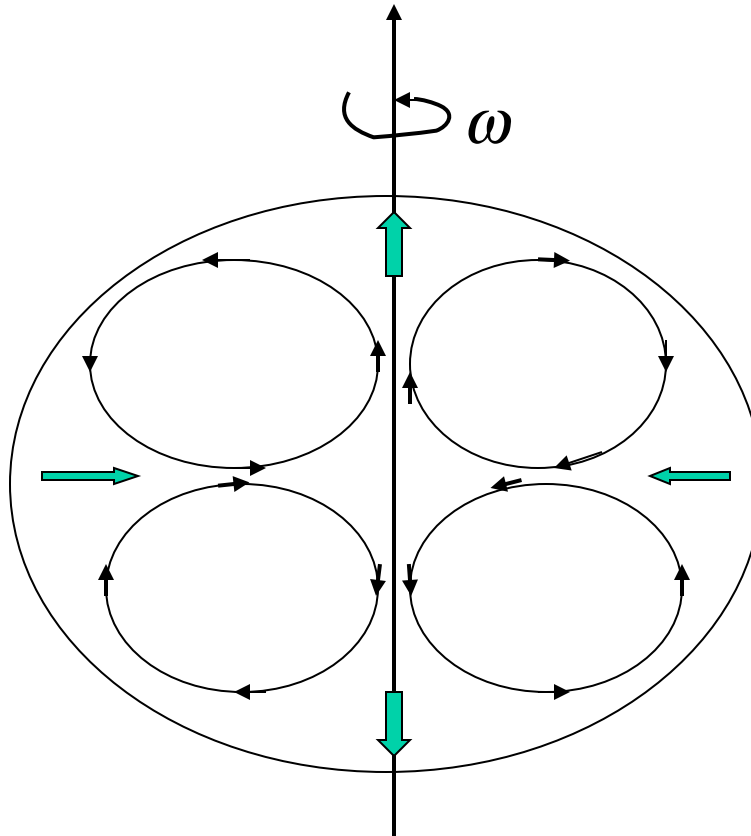


Rigid rotation



Differential rotation

Eddington-Sweet Flow Patterns



Pattern for rigid rotation is outflow along the axes, inflow in the equator.

But this can be changed, or even reversed, in the case of differential rotation,

*Mixes composition and transports angular momentum
(tends towards rigid rotation)*

As a consequence there will be regions that are heated relative to other regions at differing angles in the star resulting in some parts being buoyant compared with others. Thermal equilibrium is restored and hydrostatic equilibrium maintained if slow mixing occurs.

For rigid rotation and constant composition, the flows have the pattern shown on the previous page.

The time scale for the mixing is basically the time scale for the structure to respond to a thermal imbalance, i.e., the Kelvin Helmholtz time scale, decremented by a factor that is a measure of the importance of centrifugal force with respect to gravity.

$$\tau_{ES} \approx \frac{\tau_{KH}}{\chi}$$

$$\left(\frac{v_{rot}}{v_{esc}} \right)^2 = \frac{\omega^2 r^2 r}{2Gm} = \frac{3\omega^2}{8\pi G \bar{\rho}}$$

$$\tau_{KH} \approx \frac{GM^2}{RL} \quad \chi \approx \frac{\omega^2}{2\pi G \bar{\rho}} \sim \left(\frac{2\pi \tau_{ff}}{\tau_{rot}} \right)^2$$

→ 1 for rotational break up

For the sun, $\tau_{\text{KH}} \approx 20 \text{ My}$, $\bar{\rho} = 1.4 \text{ gm cm}^{-3}$, and the rotational period is 28 days. So $\omega \approx 3 \times 10^{-6} \text{ sec}^{-1}$, so $\chi \sim 10^{-5}$, and the Eddington Sweet time scale is about 10^{12} years, i.e., it is unimportant. It can become more important near the surface though as the density decreases (Kippenhahn 42.36)

For a $20 M_{\odot}$ star, the Kelvin Helmholtz time scale relative to the nuclear lifetime is about three times greater. More importantly, because of rapid rotation, χ is not so much less than 1. Eddington Sweet circulation is very important in massive stars.

It is more complex however in the case of differential rotation and is inhibited by radially decreasing gradients in \bar{A} . *The latter makes its effect particularly uncertain, and also keeps the stars from completely mixing on the main sequence in the general case.*

Other instabilities that lead to mixing and the transport of angular momentum: See Heger et al, *ApJ*, **528**, 368 (2000) Collins, *Structure of Distorted Stars*, Chap 7.3,7.4; Maeder's text

dynamical shear

energy available from shear adequate to (dynamically) overturn a layer. Must do work against gravity and any compositional barrier.

secular shear

Goldreich-Schubert-Fricke instability

Eddington-Sweet circulation

Solberg-Høiland instability

(Endal & Sophia 1978,
Pinsonneault, Kawaler, Sophia, Demarque 1989)

Eddington-Sweet and shear dominate.

$\frac{\partial j}{\partial r} > 0$ for stability

All instabilities will be modified by the presence of composition gradients

- **Dynamical shear**

sufficient energy in shear to power an overturn and do the necessary work against gravity

- **Secular shear**

same as dynamical shear but on a thermal time scale. Unstable if sufficient energy for overturn after heat transport into or out of radial perturbations. Usually a more relaxed criterion for instability.

- **Goldreich-Schubert-Fricke**

Axisymmetric perturbations will be unstable in a chemically

homogeneous region if $\frac{dj}{dr} \leq 0$ *or* $\frac{d\omega}{dz} \neq 0$

- **Solberg Hoiland**

Like a modified criterion for convection including rotational forces.

Unstable if an adiabatically displaced element has a net force (gravity plus centrifugal force plus buoyancy) directed along the displacement

$$\text{Stability if } \frac{g}{\rho} \left[\left(\frac{d\rho}{dr} \right)_{ad}^{\text{LeDoux}} - \frac{d\rho}{dr} \right] + \frac{1}{r^3} \frac{d}{dr} (r^2 \omega)^2 \geq 0$$

Some historic calculations including angular momentum transport:

Kippenhan et al., *A&A*, **5**, 155, (1970)

Endal & Sofia, *ApJ*, **210**, 184, (1976) and **220**, 279 (1978)

artificial rotation profiles and no transport (76) or large μ -barriers (78)

Pinsonneault *et al*, *ApJ*, **38**, 424, (1989)

the sun; improved estimates and formalism

Maeder & Zahn, *A&A*, **334**, 1000 (1998)

More realistic transport, H, He burning only

Heger, Langer, & Woosley, *ApJ*, **528**, 368, (2000)

First “realistic” treatment of advanced stages of evolution

Maeder & Meynet, *A&A*, **373**, 555, (2001)

Heger, Woosley, and Spruit, *ApJ*, **626**, 350, (2005)

First inclusion of magnetic torques in stellar model

Surface abundances studied by:

Ekstrom et al , *A&A*, **537**, 146, (2012)

Meynet & Maeder, *A&A*, **361**, 101, (2000)

Heger & Langer, *ApJ*, **544**, 1016, (2000)

In massive stars, Eddington Sweet dominates on the main sequence and keeps the whole star near rigid rotation. Later dynamical shear dominates in the interior.

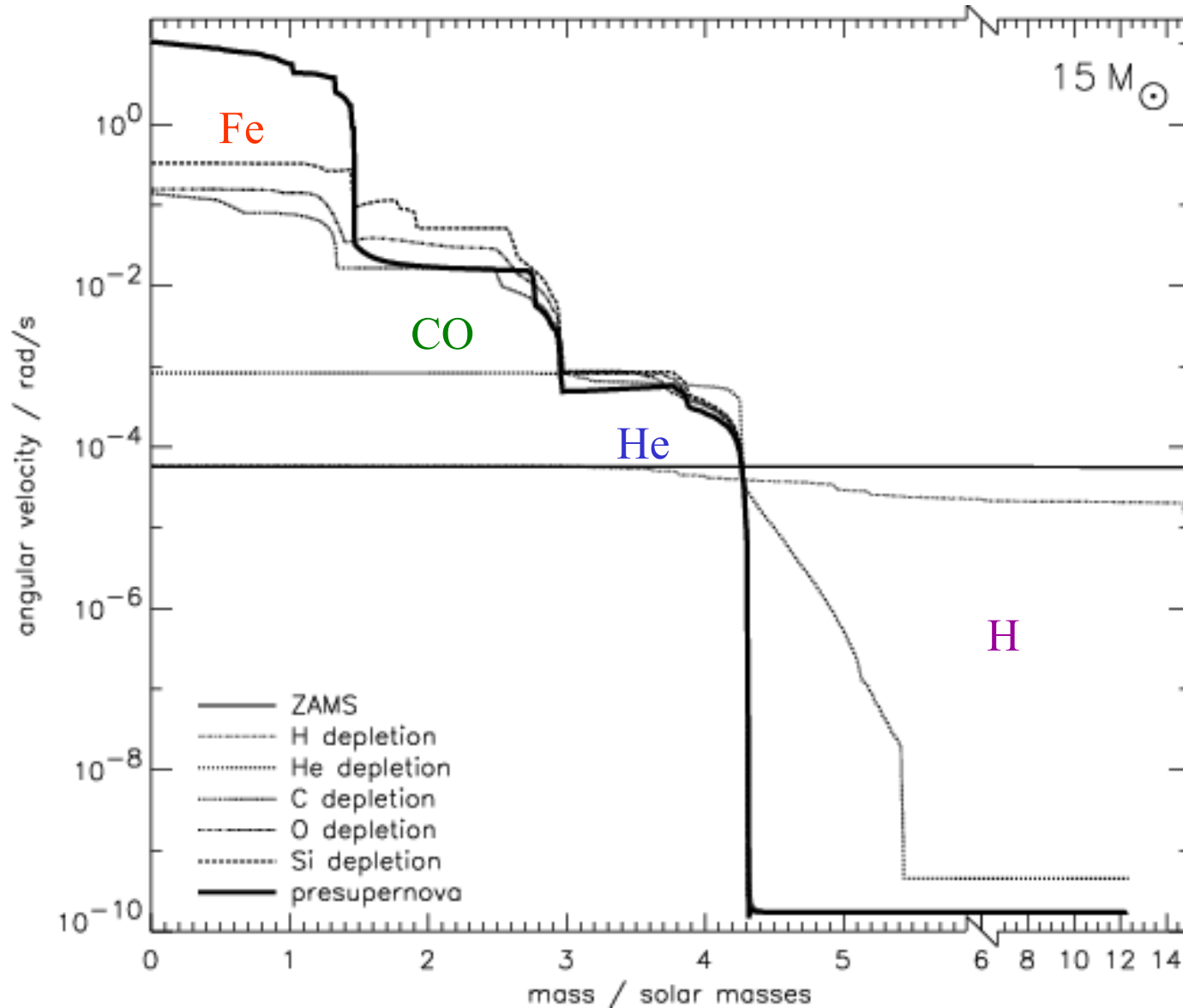
Results:

- Fragile elements like Li, Be, B destroyed to a greater extent when rotational mixing is included. More rotation, more destruction.
- Higher mass loss
- Initially luminosities are lower (because g is lower) in rotating models. later luminosity is higher because He-core is larger
- Broadening of the main sequence; longer main sequence lifetime
- More evidence of CN processing in rotating models. He, ^{13}C , ^{14}N , ^{17}O , ^{23}Na , and ^{26}Al are enhanced in rapidly rotating stars while ^{12}C , ^{15}N , $^{16,18}\text{O}$, and ^{19}F are depleted.
- Decrease in minimum mass for WR star formation.

These predictions are in good accord with what is observed.

Evolution Including Rotation

Heger, Langer, and Woosley (2000), *ApJ*, **528**, 368



20 M_{\odot} Near Hydrogen Depletion

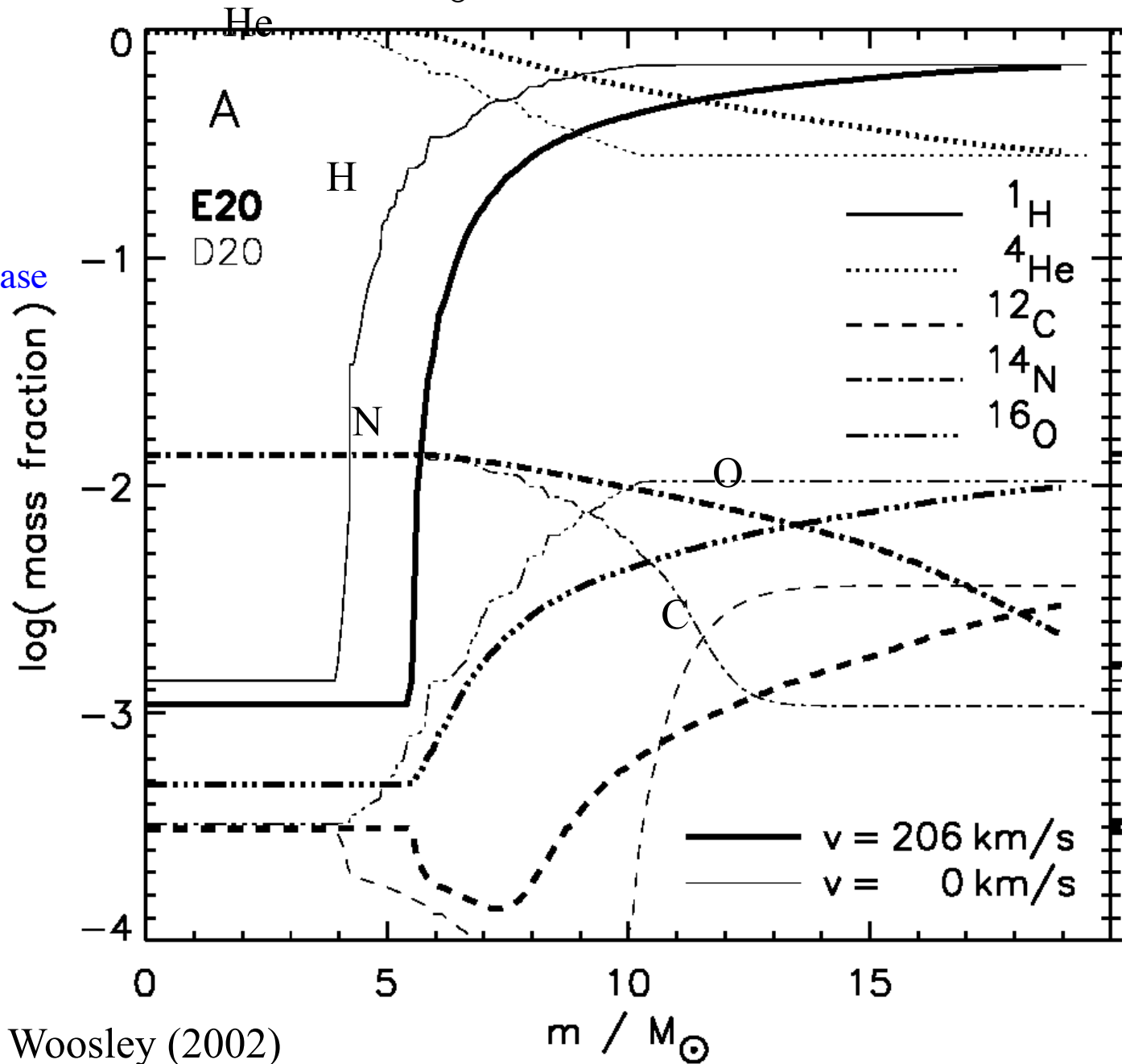
He \uparrow (He core larger)

C same but \downarrow

N \uparrow

O same but \downarrow

Mass loss would increase
the effects



Final angular momentum distribution is important to:

- Determine the physics of core collapse and explosion
- Determine the rotation rate and magnetic field strength of pulsars
- Determine the viability of models for gamma-ray bursts.

B-fields

The magnetic torques are also important for this. The magnitude of the torque is approximately:

$$S \sim \frac{B_r B_\phi}{4\pi} \quad \frac{dL}{dt} \sim S R^3 \quad \text{with } L \text{ the angular momentum}$$

Maeder - eq. 13-94

$$S = \frac{1}{4\pi} \vec{r} \times (\vec{\nabla} \times \vec{B}) \times \vec{B}$$

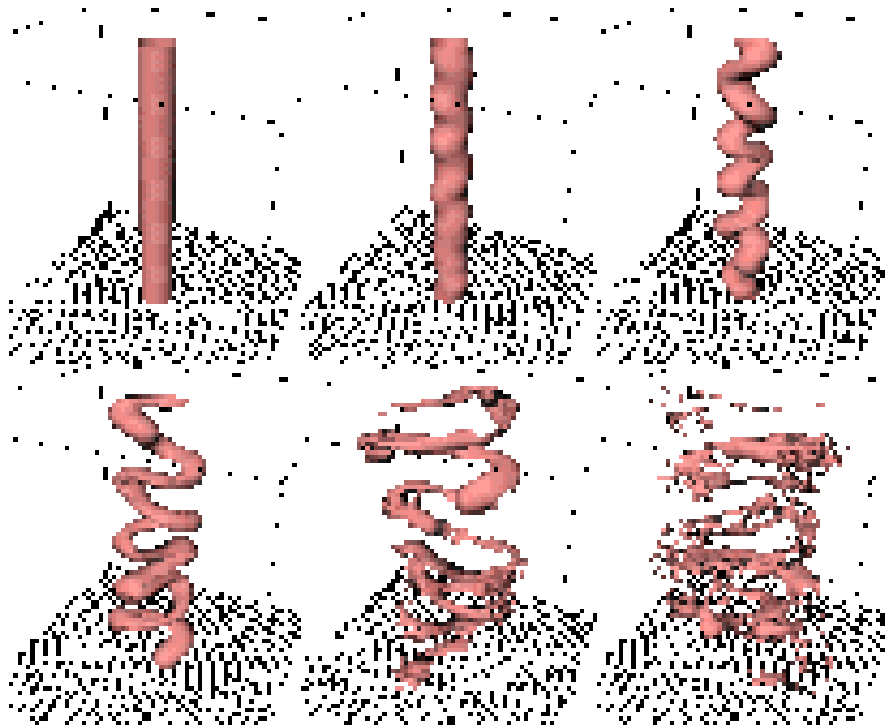
Spruit and Phinney, *Nature*, **393**, 139, (1998)

Assumed B_r approximately equal B_ϕ and that B_ϕ was from differential winding. Got nearly stationary helium cores after red giant formation. Pulsars get rotation from “kicks”.

Spruit, *A&A*, **349**, 189, (1999) and **381**, 923, (2002)

B_r given by currents from an interchange instability. Much smaller than B_ϕ . Torques greatly reduced

Heger, Woosley, and Spruit, *ApJ*, **626**, 350, (2005); Woosley and Heger, *ApJ*, **637**, 914 (2006) ; Yoon and Langer, *A&A*, **443**, 643 (2006) implemented these in stellar models.



$$\text{Torque} \propto B_r B_\phi$$

B_ϕ from differential winding

B_r from Tayler-Spruit dynamo

Spruit (2002, 2006)

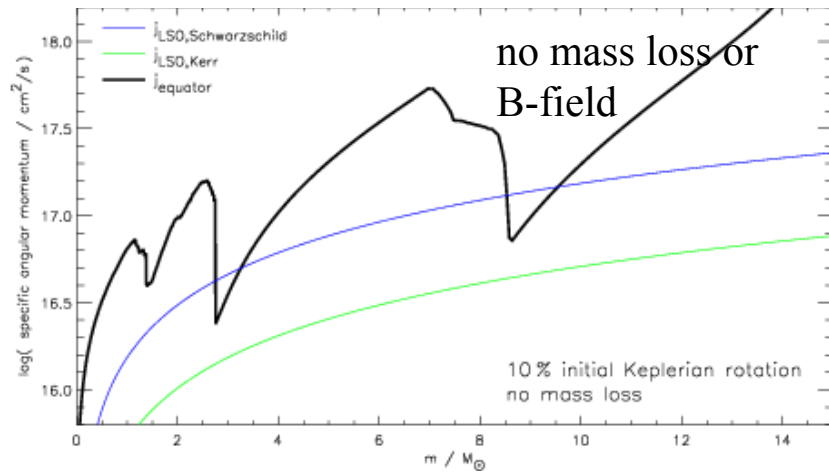
Braithwaite (2006)

Denissenkov and Pinsonneault
(2006)

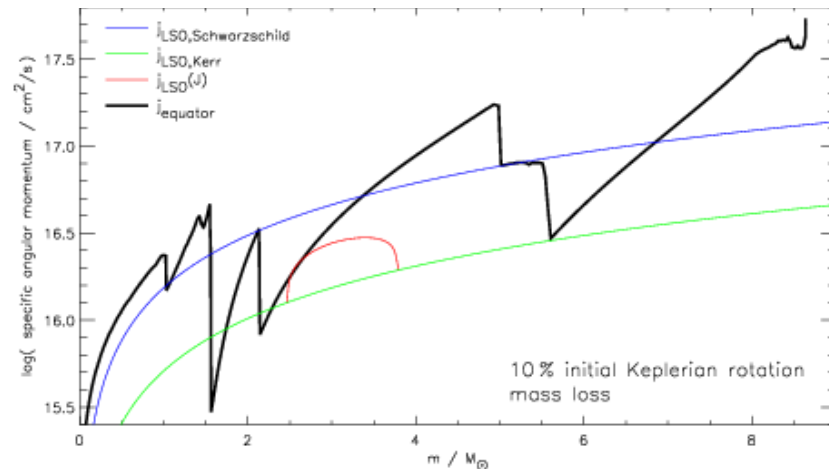
Zahn, Brun, and Mathis
(2007)

*Approximately confirmed for
white dwarf spins (Suijs et al
2008)*

"Any purely poloidal field should be unstable to instabilities on the magnetic axis of the star" (Tayler 1973)



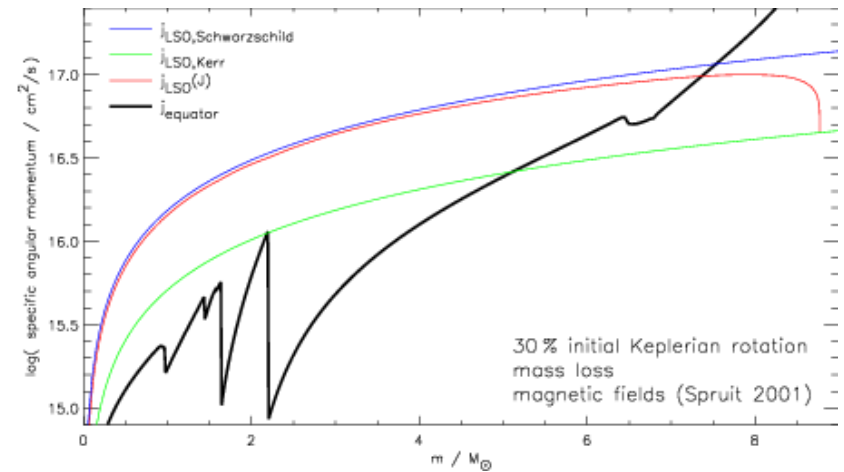
15 solar mass helium core born rotating rigidly at f times break up



with mass loss

If include WR mass loss and magnetic fields the answer is greatly altered....

15 M_{\odot} rotating helium star



with mass loss and B-fields

Stellar evolution including approximate magnetic torques gives slow rotation for common supernova progenitors. (solar metallicity)

Table 4: Pulsar Rotation Rate With Variable Remnant Mass^a

Mass	Baryon ^b (M _⊙)	Gravitational ^c (M _⊙)	$J(M_{\text{bary}})$ (10 ⁴⁷ erg s)	BE (10 ⁵³ erg)	Period ^d (ms)
12 M _⊙	1.38	1.26	5.2	2.3	15
15 M _⊙	1.47	1.33	7.5	2.5	11
20 M _⊙	1.71	1.52	14	3.4	7.0
25 M _⊙	1.88	1.66	17	4.1	6.3
35 M _⊙ ^e	2.30	1.97	41	6.0	3.0

magnetar progenitor?

^a Assuming a constant radius of 12 km and a moment of inertia $0.35MR^2$ (Lattimer & Prakash 2001)

^b Mass before collapse where specific entropy is $4k_B/\text{baryon}$

^c Mass corrected for neutrino losses

^d Not corrected for angular momentum carried away by neutrinos

^e Became a Wolf-Rayet star during helium burning

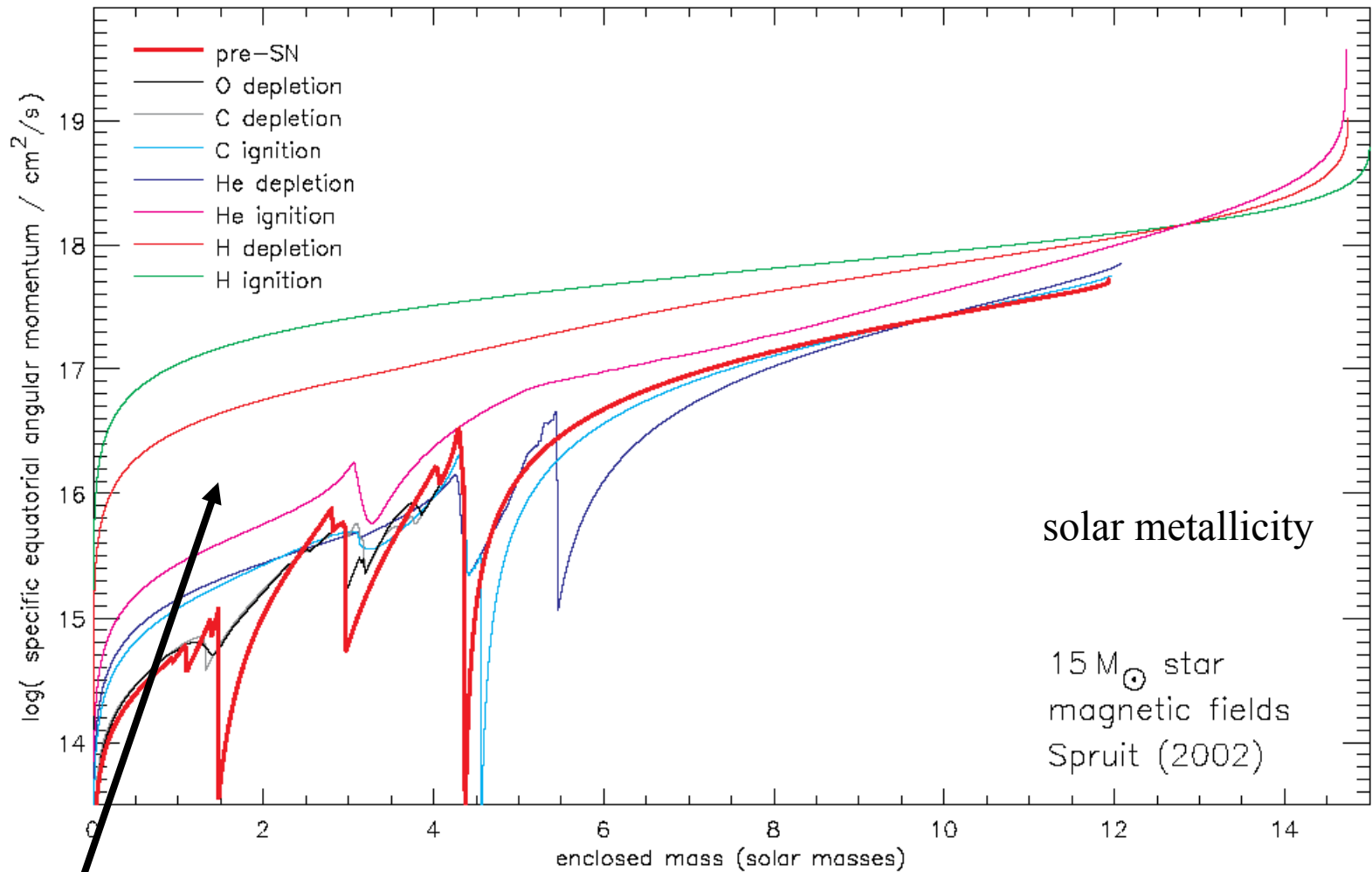
Heger, Woosley, & Spruit (2004)
using magnetic torques as derived in
Spruit (2002)

This is consistent with what is estimated for young pulsars

Table 5: Periods and Angular Momentum Estimates for Observed Young Pulsars

pulsar	current (ms)	initial (ms)	J_o (erg s)
PSR J0537-6910 (N157B, LMC)	16	~10	8.8×10^{47}
PSR B0531+21 (crab)	33	21	4.2×10^{47}
PSR B0540-69 (LMC)	50	39	2.3×10^{47}
PSR B1509-58	150	20	4.4×10^{47}

from HWS04



Much of the spin down occurs as the star evolves from H depletion to He ignition, i.e. forming a red supergiant.

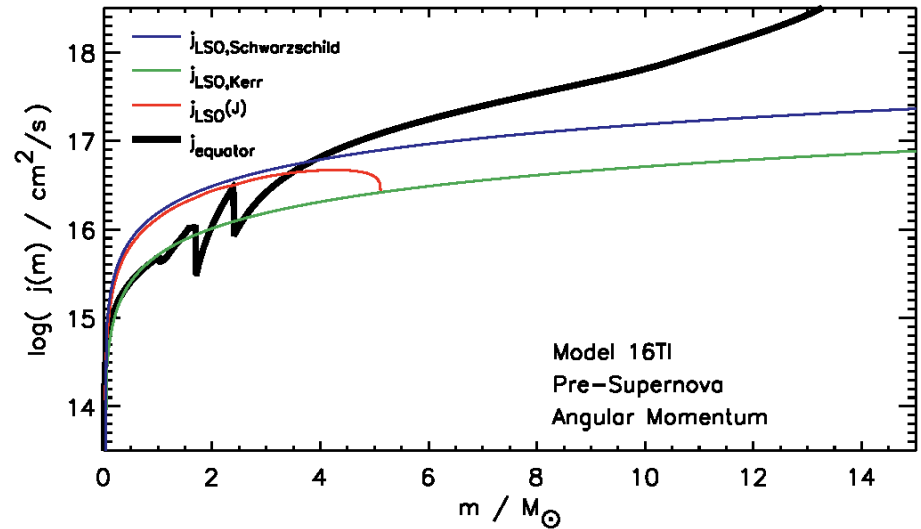
Heger, Woosley, & Spruit (2004)

Chemically Homogeneous Evolution

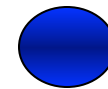
- If rotationally induced chemical mixing during the main sequence occurs faster than the built-up of chemical gradients due to nuclear fusion the star evolves chemically homogeneous (Maeder, 1987)

$$\frac{\tau_{ES}}{\tau_{MS}} < 1$$

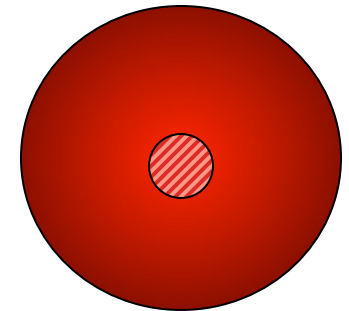
- The star evolves blueward and becomes directly a Wolf Rayet (no RSG phase). This is because the envelope and the core are mixed by the meridional circulation -> **no Hydrogen envelope**
- Because the star is not experiencing the RSG phase it retains an **higher angular momentum in the core** (Woosley and Heger 2006; Yoon & Langer, 2006)



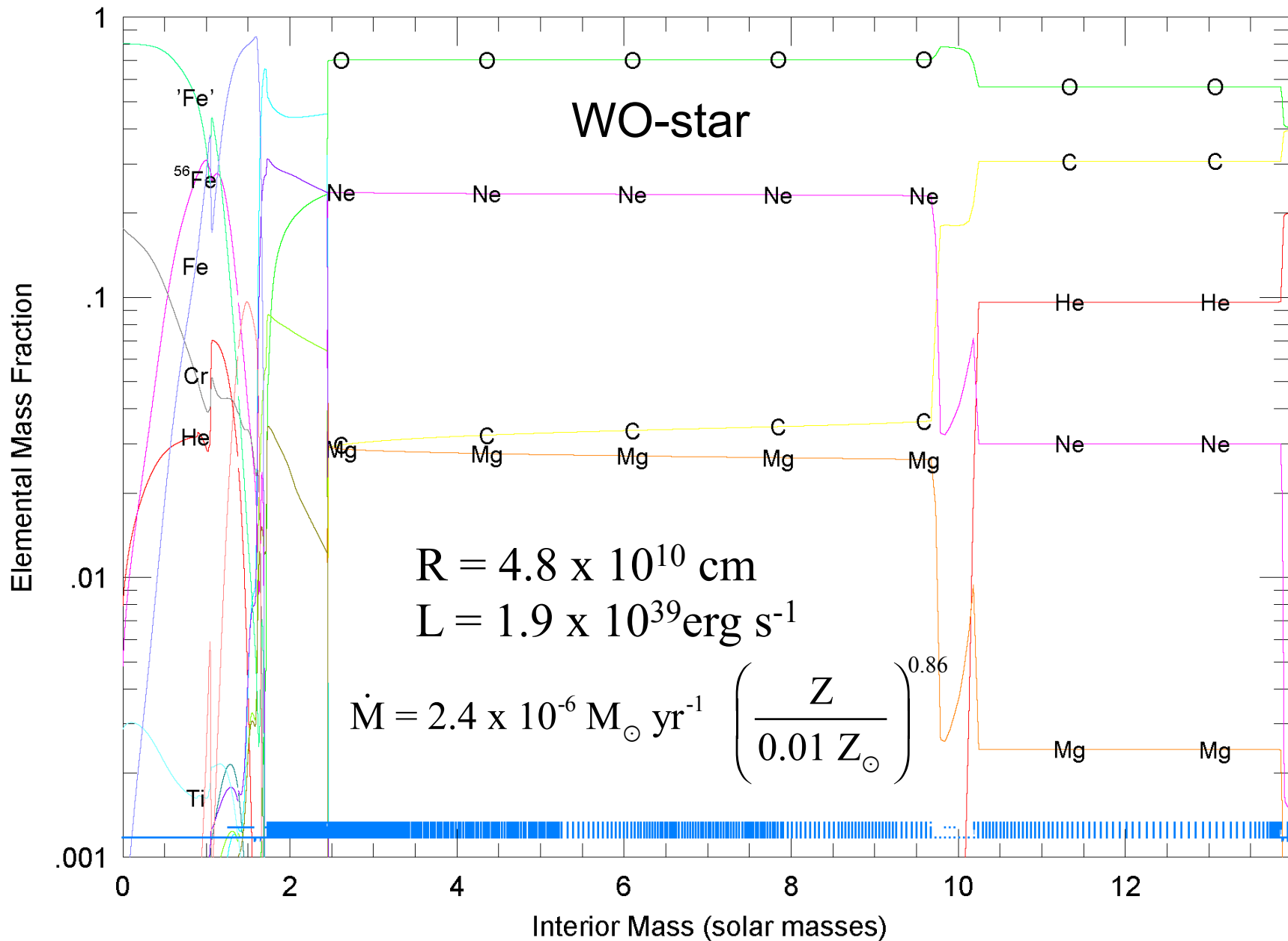
Woosley and Heger (2006)



R~1 R_{sun}



R~1000 R_{sun}



Derived from $16 M_{\odot}$ star with rapid rotation and low Z